Forward Error Correction for Low-Delay Interactive Applications

Ahmed Badr, *Member, IEEE*, Ashish Khisti, *Member, IEEE*,
Wai-tian Tan, *Member, IEEE*, and John Apostolopoulos, *Fellow IEEE*

Abstract

Many current and emerging applications require low-latency communication, including interactive voice and video communication, multi-player gaming, multi-person augmented reality and virtual reality, and various Internet of Things applications. Forward Error Correction (FEC) codes for low-delay interactive applications have several distinguishing characteristics from traditional FEC. The encoding and decoding operations must process a stream of data packets in a sequential fashion. Strict latency constraints limit the use of long block lengths, interleaving, or large buffers. Furthermore these codes must achieve fast recovery from burst losses and yet be robust to random losses.

This tutorial paper provides a survey of FEC for low-delay interactive applications. We provide several illustrative examples that explain why off-the-shelf codes such as Reed-Solomon Codes, Digital Fountain Codes, or Random-Linear Convolutional Codes do not provide ideal error correction for such applications. We then introduce some recently proposed FEC for streaming, discuss their properties, and quantify their performance gains both through illustrative examples as well as through simulations over statistical channel models and real packet traces.

Index Terms

Streaming Communication Systems, Delay Constrained Communication, Application Layer Forward Error Correction, Burst Erasure Channels, Low Latency.

Ahmed Badr and Ashish Khisti are with the School of Electrical and Computer Engineering, University of Toronto, Toronto, ON, M5S 3G4 Canada (e-mail: {abadr,akhisti}@ece.utoronto.ca). Wai-tian Tan and John Apostolopoulos are with Cisco Systems, CA {dtan2,johnapos}@cisco.com.

This work was supported by a discovery grant from National Science and Engineering Research Council of Canada, Hewlett Packard through a HP-IRP Award, Cisco Systems, and an Ontario Early Researcher Award.

I. Introduction

In the last decade we have witnessed an explosive demand for multimedia streaming applications. A recent study [1] predicts that IP Video alone will constitute 79% of all the consumer Internet traffic in 2018. Some commonly used applications include VoIP, video-on-demand (VoD), video conferencing, desktop sharing and interactive network gaming. Emerging applications that require low-latency include augmented reality, virtual reality, and various Internet of Things (IoT) applications involving control loops for industrial processes. The underlying communication network for these applications must support high reliability, low latency, and preferably in-order delivery of source packets. Furthermore it must include wireless links, that are subject to noise, fading, mobility and interference. To combat such impairments various error-control mechanisms must be implemented.

In the physical layer of wireless systems powerful error-correcting codes such as turbo codes are used to combat short-term fast fading and white Gaussian noise. These codes cannot always recover from other sources of impairments such as slow fading, buffer overflow, congestion or interference, which cause packet losses at the application layer. It is well known that certain loss patterns such as burst losses can cause a significant deterioration in both audio and video streaming [2], [3]. It therefore becomes necessary to develop error-control techniques at the application layer to mitigate the effect of packet losses.

Error control mechanisms at the application layer can be divided into two classes — error concealment and error correction. Error concealment techniques such as interpolation are used to mask the effect of missing source packets. These techniques are outside the scope of this tutorial. Error correction techniques such as retransmission and forward error correction (FEC) are used to achieve reliable transmission over communication links. In retransmission based schemes, e.g., Automatic Repeat reQuest (ARQ), if the transmitter receives no acknowledgment for a given packet within a certain time, the packet is retransmitted to the receiver. While retransmission is a simple and effective means of error correction, it requires point-to-point communication, a feedback channel and low round-trip delay. The round-trip delay depends on a number of factors such as the distance between the source and destination, the number of nodes that must be traversed in-between, the processing delay at each node and the speed of the links [4]. It is valuable to remember that even if we operate at the speed of light without any other delays we still have end-to-end delay issues. At the speed of light the time required to travel along the earth's circumference is 133 ms. This would correspond to the theoretical minimum round-trip delay between two diametrically opposite points on the earth's circumference. The original one-way delay of the packet transmission plus the round-trip delay from ARQ can produce a minimum latency of about 200 ms. In practice this theoretical delay would be longer due to the non-ideal refractive index of the optical fibre and non-direct paths between the nodes. On the other hand, the ITU recommendation states that the end-to-end latency in interactive voice and video applications must be less than 150 ms [5]–[7]. Clearly, even in the ideal case, the distances involved and the application constraints preclude the sole use of retransmissions. Applications such as augmented reality and virtual reality have even tighter delay constraints. For example, the time from a user's motion until when it should be reflected in the user's display (commonly referred to as "motion to photon latency") needs to be less than 20 ms to provide the experience of presence. Similarly, IoT applications that involve control feedback loops may require 1 ms or sub-ms latency, depending on the control loop requirements — orders of magnitude tighter delay constraints than traditional applications. In addition, support for ultra low latency wireless services (ms level) are defined as a requirement for 5G cellular systems [8].

A common alternative to retransmission is Forward Error Correction (FEC), where redundant data are derived from the original data using techniques from coding theory. Error correcting codes such as Low-Density Parity-Check (LDPC) and Digital Fountain codes [9], [10] are recommended in Internet Engineering Task Force (IETF) Real-Time Transport Protocol (RTP) profiles for non-interactive streaming applications. These codes operate over long block lengths, typically a few thousand symbols and are thus suitable in applications when the delay constraints are not stringent. In contrast FEC used in interactive applications are often constrained to have short block lengths due to the delay constraints. Nevertheless real-world interactive audio and video conferencing applications such as Skype [11], are known to use FEC with significant advantages.

In this paper we will take a principled approach towards understanding ideal FEC for low-delay interactive applications. In these applications the FEC-encoding and FEC-decoding operations must happen sequentially on the source and channel streams respectively. Furthermore certain erasure patterns such as burst losses can severely degrade the performance [2], [3], [11]. To illustrate the effect of burst losses, consider the two types of packet-loss sequences in Fig. 1.

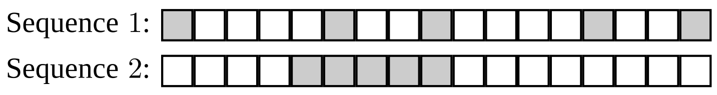

Fig. 1: Two examples of erasure sequences, which have the same number of erasures but different erasure patterns. The shaded boxes denote the erasures while the white boxes denote packet reception. In sequence 1 the erasures are mostly isolated, while in sequence 2 they occur in a single burst. One can use a short $(3, 2)$ RS code to recover for sequence 1, but a longer $(15, 10)$ RS code is required over sequence 2, resulting in a higher delay.

Note that both of these sequences have the same fraction of lost packets. Sequence 1 in Fig. 1 corresponds to packet losses that are well separated, while sequence 2 corresponds to packet losses in a burst. In the former case, a short-block code can be used for error correction. For example a $(3, 2)$ Reed-Solomon (RS) code [12] will guarantee that all the source packets that have been erased on link 1 will be recovered. This is possible as there is at-most one erasure among any three consecutive packets. For sequence 2 in Fig. 1, a $(3, 2)$ block code cannot be used to recover the burst loss of 5 packets. We will have to use a longer $(15, 10)$ RS code to recover all the erased source packets, while also maintaining the same overhead as in sequence 1. However, the delay incurred with this code is considerably higher than the previous case. Thus the dynamics of packet loss patterns, and not just the average fraction of losses, must be considered in streaming applications.

We will discuss coding techniques that can repair from burst losses with a much shorter delay than RS codes. We will also see that codes that are optimal for burst losses in terms of minimizing the delay are rather sensitive to other loss patterns. In practice communication links introduce both types of erasure patterns illustrated in Fig. 1. Thus we will discuss coding schemes that enable *fast* recovery from burst losses, and are also robust to isolated losses [13]–[15].

In the rest of the paper, Section II provides a case study of a streaming setup and examines the properties of various error correction codes including Reed-Solomon Block Codes, Random Linear Convolutional (RLC) Codes, Repetition Codes, as well as some variants of these such as shifted-Repetition, shifted-RLC, Concatenated and Dual-Delay codes. We examine the error correction ability of these codes against burst losses, as well as arbitrary loss patterns and explain how the proposed variants outperform the baseline schemes. In Section III we explain how these constructions can be generalized to obtain state-of–the-art low-delay FEC for channels with burst and isolated losses, while Section IV summarizes the literature on Streaming Codes till date.

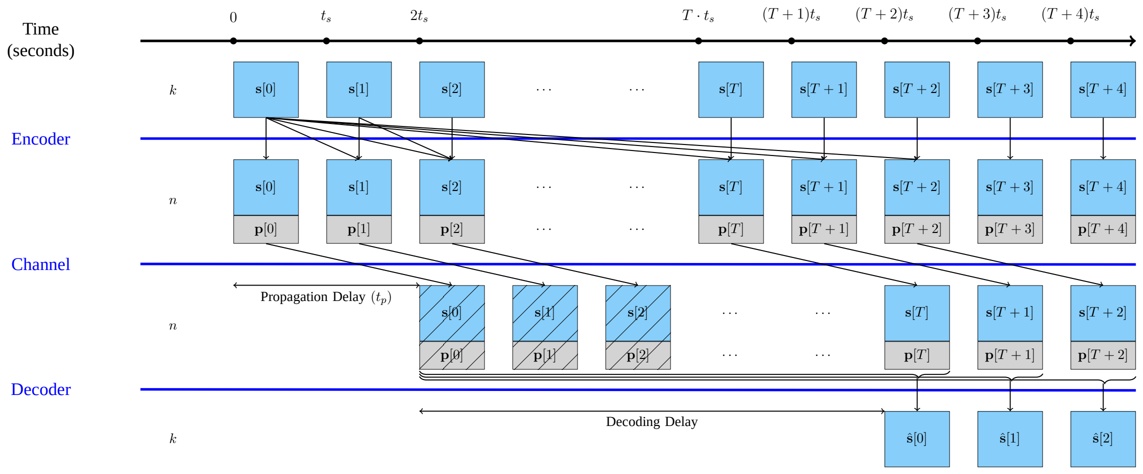
Time (seconds)
0
t_s
$2t_s$
$T \cdot t_s$
$(T+1)t_s$
$(T+2)t_s$
$(T+3)t_s$
$(T+4)t_s$
k
$\mathbf{s}[0]$ $\mathbf{s}[1]$ $\mathbf{s}[2]$ ⋯ ⋯ $\mathbf{s}[T]$ $\mathbf{s}[T+1]$ $\mathbf{s}[T+2]$ $\mathbf{s}[T+3]$ $\mathbf{s}[T+4]$
Encoder
n
$\mathbf{p}[0]$ $\mathbf{p}[1]$ $\mathbf{p}[2]$ ⋯ ⋯ $\mathbf{p}[T]$ $\mathbf{p}[T+1]$ $\mathbf{p}[T+2]$ $\mathbf{p}[T+3]$ $\mathbf{p}[T+4]$
Channel
Propagation Delay (t_p)
Decoder
Decoding Delay
$\hat{\mathbf{s}}[0]$ $\hat{\mathbf{s}}[1]$ $\hat{\mathbf{s}}[2]$

Fig. 2: The source stream $\mathbf{s}[t]$ for $t \geq 0$ is encoded to a channel stream $\mathbf{x}[t]$ which is transmitted over an erasure channel. The decoder tolerates a maximum delay of T packets.

Section V provides simulation results over Gilbert-Elliott channel models and real packet traces and conclusions are presented in Section VI.

II. Case Study: Why Traditional FEC is Not Enough?

In this section we study the performance of various error correcting codes in a streaming setup via an example. In order to provide a common point of comparison we focus on the streaming setup shown in Fig. 2. In this model a source packet $\mathbf{s}[t]$ for $t = 0, 1, 2, \ldots$ arrives at the FEC encoder every t_s seconds, i.e., $\mathbf{s}[t]$ arrives at time $t \cdot t_s$ seconds. For simplicity, we will assume that each source packet is of the same size and consists of k symbols. The encoder generates a channel packet $\mathbf{x}[t]$ of size n symbols and transmits it in the interval $[t \cdot t_s, (t+1) \cdot t_s)$. The encoding function is causal:

$$\mathbf{x}[t] = f_t\left(\mathbf{s}[t-m], \ldots, \mathbf{s}[t]\right), \quad t \geq 0, \tag{1}$$

where $f_t(\cdot)$ is the encoding function at time t and m denotes the memory of the encoder. Furthermore the rate of the code is given by $R = k/n$ and its redundancy is $100(n-k)/k\%$. The communication channel considered is a *packet erasure channel*. Each transmitted packet is either erased or perfectly received at the destination. This is motivated by the fact that erroneous packets are discarded at lower layers in the communication protocol stack. In particular, the channel output at (discrete) time t is given by $\mathbf{y}[t] = \star$, if the channel introduces an erasure at time t, and by $\mathbf{y}[t] = \mathbf{x}[t]$, if it does not. Throughout this paper we will use the term *channel* to denote the packet-loss sequence, as is the convention in the literature in coding theory. In order to develop insights into the performance of different coding schemes we will focus on a simple class of channels defined below.

Definition 1 (Burst Erasure Channel)**.** *A Burst Erasure Channel with parameter B is a channel that introduces a single contiguous sequence of erasures of maximum length B, i.e., starting from some arbitrary time $j \geq 0$ and $0 \leq B' \leq B$, we have that $\mathbf{y}[t] = \star$ for $t \in [j, j+B'-1]$ and $\mathbf{y}[t] = \mathbf{x}[t]$ otherwise.*

Definition 2 (Isolated Erasure Channel)**.** *An Isolated Erasure Channel with parameter N is a channel that introduces up to N erasures in the received stream. The locations of the erasures can be arbitrary. Thus for some $0 < N' \leq N$ and $0 \leq j_1 < j_2 \ldots < j_{N'}$ we have that $\mathbf{y}[j_l] = \star$, and $\mathbf{y}[t] = \mathbf{x}[t]$ if $t \notin \{j_1, j_2, \ldots, j_{N'}\}$.*

We note that the channel models treated above are rather simple — the burst erasure model introduces a single burst of maximum length B, while the isolated erasure channel introduces a maximum of N erasures in arbitrary locations. Nevertheless there are several advantages in studying these models:

- The study of such simplified model provides first order insights into the performance of various streaming codes. For example we will see how convolutional codes are more resilient than block codes in the streaming setup.
- The analysis of these channels is a useful first step in treating more sophisticated models such as the sliding window channel models, which must be naturally considered in streaming scenarios [13], [14].
- We will see that the insights obtained through the study of such channels will be useful in interpreting the simulation results over the Gilbert-Elliot model and real packet traces treated in Section V.

As shown in Fig. 2, the decoder tolerates a maximum delay of T packets, i.e.,

$$\hat{\mathbf{s}}[t] = \gamma_t(\mathbf{y}[0], \ldots, \mathbf{y}[t+T]), \tag{2}$$

where $\gamma_t(\cdot)$ designates the decoding function at time t. The source packet $\mathbf{s}[t]$ is declared *lost* if $\hat{\mathbf{s}}[t] \neq \mathbf{s}[t]$. Note that a delay of T packets in our model is equivalent to an actual delay of

$(T \cdot t_s + t_p)$ seconds, where t_s is the inter-packet arrival time and t_p is the propagation delay in Fig. 2. In the rest of the paper we will consider the delay in terms of packets, and the time index will refer to the discrete time.

Remark 1. *The constructions considered in Fig. 2 are systematic codes, i.e., each channel packet can be expressed as* $\mathbf{x}[t] = (\mathbf{s}[t], \mathbf{p}[t])$, *where* $\mathbf{p}[t]$ *is the parity-check packet consisting of* $(n-k)$ *symbols. All codes that we will consider in this paper will be systematic codes. This will guarantee that whenever a channel packet is received the underlying source packet is immediately recovered with zero delay. Furthermore all codes we consider will be linear codes, i.e., the parity-check symbols can be expressed as a linear combination of the source packets [16].*

Remark 2. *Note that in the setup in Fig. 2 the parity-check packets* $\mathbf{p}[t]$ *are not transmitted as separate packets but are* appended *to the source packets before transmission. This reduces the number of packets transmitted over the channel. Such an approach is desirable in practical wireless networks such as 802.11, where channel contention overhead is significant. Nevertheless most of the insights developed for our proposed model also apply, with minor variations, to the case when the parity-check packets are transmitted separately. Advantages of using separate FEC streams include wider compatibility, where media stream can be decoded even by clients that do not understand FEC.*

A. Summary of Coding Schemes

We briefly summarize the different code constructions that will be discussed in the paper. As illustrated in Fig. 3, the coding schemes we consider can be broadly classified into two categories (i) traditional FEC and (ii) streaming codes. In the former category we will discuss three off-the-shelf coding schemes: Reed-Solomon codes, Rateless codes and Random Linear Convolutional codes in sections II-B, II-C and II-D. A common feature of these codes is that following a loss pattern, the decoder must collect enough parity-checks so that it can invert the resulting system of equations and simultaneously recover all the missing source packets. For example when the rate of the code is $R = 1/2$, so that the size of each parity-check equals that of the source packet, the decoder must collect as many parity-check packets as the missing source packets to recover them. In the special case of the burst erasure channel with burst length of B and $R = 1/2$, this results in a delay of $T = 2B$.

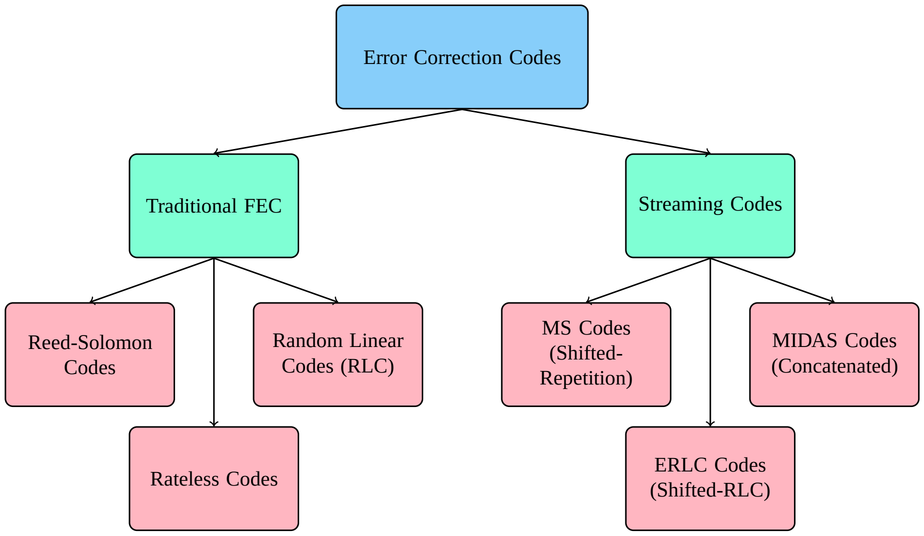

Fig. 3: Summary of different coding schemes in the streaming setup. The traditional FEC are discussed in Section II. The rate-$1/2$ streaming codes — shifted-Repetition, shifted-RLC and Concatenated Codes — are also discussed in Section II. The shifted-Repetition code provides optimal burst error correction in the streaming setup, while the shifted-RLC and Concatenated Codes are a robust extension of these codes. Their respective generalizations — MS codes, ERLC codes and MIDAS codes are discussed in Section III.

One can significantly improve upon the performance of traditional FEC over burst erasure channels. Such constructions will be referred to as *streaming codes* in this paper. Unlike traditional FEC, they do not force simultaneous recovery of all the source packets. Instead the construction of parity-checks is such that the older source packets with earlier deadlines are recovered before the later source packets. The minimum delay achieved by this method is $T = B$, when $R = 1/2$.

In Fig. 4 we provide a comparison between traditional FEC and streaming codes. We sketch the maximum correctable burst length on the x-axis and the resulting delay for different codes on the y-axis. The rate of all codes is fixed to $R = 1/2$. As we discussed, when the burst length equals B the minimum delay for traditional FEC is $T = 2B$, which is shown by the blue line in the figure. The associated region $T \geq 2B$ is shaded light blue. In contrast the minimum delay achieved by streaming codes is $T = B$ and is shown by the red line. Thus the longer the burst length, the higher will be the gain provided by streaming codes. As we will see the codes achieving minimum delay over burst loss channels are sensitive to other erasure patterns. Thus in practice one must develop robust extensions that are also resilient to isolated erasure patterns. Such codes will require slightly larger delays than $T = B$, and will achieve a performance in the light red region shown in Fig. 4. We discuss three such constructions,

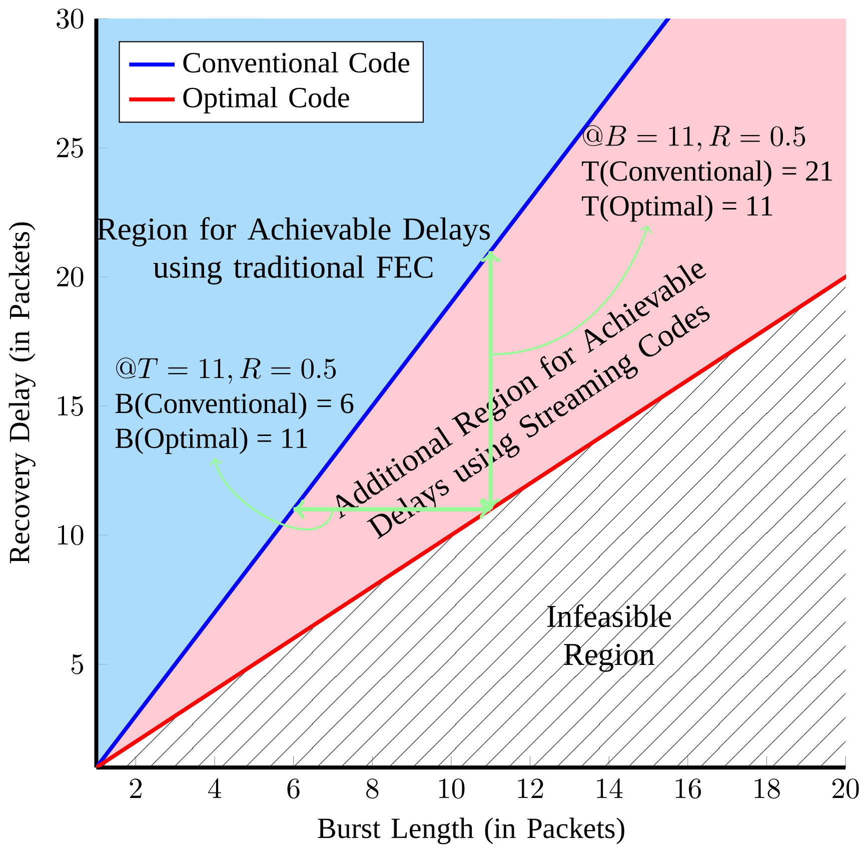

Fig. 4: Achievable delays for erasure recovery of different burst lengths using FEC at rate $1/2$. The solid red-line shows the minimum delay that can be achieved for a given burst length. The delay below this threshold cannot be achieved by any code. The blue region shows the delay achieved by traditional FEC that perform simultaneous recovery of the source packets. Streaming codes that perform sequential recovery can achieve delay in the red region.

shifted-RLC codes, Concatenated codes and dual-delay codes in Sections II-F, II-G and II-H respectively. The corresponding generalizations to arbitrary rates are discussed in Section III.

B. Reed-Solomon Block Codes

An (n, k) block code operates on k source packets and generates $n > k$ packets. Hence, the rate of a (n, k) code is given by k/n. Systematic codes are a class of block codes where the first k packets of the codeword are the source packets, whereas the last $n - k$ are called parity-check packets. Reed-Solomon (RS) [12], [16] codes are the most commonly used block codes. These codes belong to the class of Maximum Distance Separable (MDS) codes which guarantee the recovery of the maximum number of packet losses for a given redundancy. An (n, k) RS code can recover up to $n - k$ erased packets in any codeword of length n.

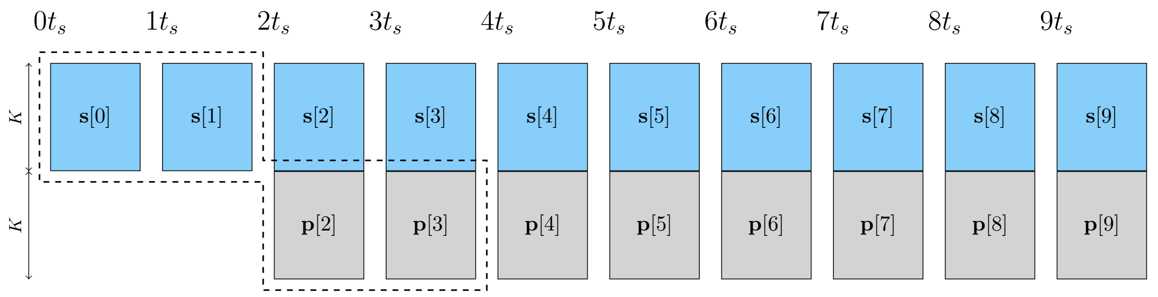

Fig. 5: $(4,2)$ RS Code applied to a streaming setup. The parity-check packets $\mathbf{p}[2]$ and $\mathbf{p}[3]$ are generated from $\mathbf{s}[0]$ and $\mathbf{s}[1]$, but sent in the next block.

While a (n,k) block code does not directly fit into the streaming setup, it can be easily adapted as discussed below. The stream of source packets is logically split into segments each of size k. A (n,k) block code is then applied to each segment to generate $n-k$ parity-check packets. These parity-check packets are then transmitted together with the source packets in the *next block* of k packets. This construction is particularly simple for $R = 1/2$, which is the case treated in this section. For the case of general rates, we refer the reader to [17].

In Fig. 5, a $(4,2)$ RS code is applied to each group of two consecutive source packets to generate two parity-check packets. For example in the first block we generate

$$(\mathbf{s}[0], \mathbf{s}[1]) \xrightarrow{(4,2)\ RS\ Code} (\mathbf{s}[0], \mathbf{s}[1], \mathbf{p}[2], \mathbf{p}[3]). \tag{3}$$

The resulting parity-check packets $(\mathbf{p}[2], \mathbf{p}[3])$ are transmitted in the next block, by appending them to $\mathbf{s}[2]$ and $\mathbf{s}[3]$ respectively. The resulting channel packets are $\mathbf{x}[2] = (\mathbf{s}[2], \mathbf{p}[2])$ and $\mathbf{x}[3] = (\mathbf{s}[3], \mathbf{p}[3])$. More generally for the group of source packets $(\mathbf{s}[2i], \mathbf{s}[2i+1])$ a $(4,2)$ RS code is applied to generate parity-checks $\mathbf{p}[2i+2]$ and $\mathbf{p}[2i+3]$, which are transmitted along with the source packets at times $t = 2i+2$ and $t = 2i+3$ respectively.

A longer $(6,3)$ RS code can be applied in an analogous fashion, by considering groups of three source packets and generating three parity-check packets, which must be transmitted in the next block of three source packets. We now discuss the error correction properties. We discuss three cases below.

- **Single Isolated Loss**: Consider a channel that introduces a single isolated erasure, i.e., $N = 1$. The $(4,2)$ RS code can recover the missing source packet with a delay no more than $T = 2$ packets. For example, if $\mathbf{x}[0]$ is lost, then the associated source packet is recovered as soon as $\mathbf{p}[2]$ is received by the decoder. In contrast the $(6,3)$ RS code can recover the missing source packet with a (worst case) delay of $T = 3$ packets.

- **Two Isolated Losses**: Next consider the case when the channel introduces up to two isolated losses. For the $(4,2)$ code it can be seen that the worst case delay happens when $\mathbf{x}[0]$ and one of either $\mathbf{x}[1]$ or $\mathbf{x}[2]$ are erased. The source packet $\mathbf{s}[0]$ can be recovered from $\mathbf{p}[3]$ resulting in a delay of $T = 3$ packets. Similarly for the $(6,3)$ code the worst case delay with two isolated losses is $T = 4$. It will happen for example if $\mathbf{x}[0]$ and $\mathbf{x}[3]$ are erased, so that the decoder must wait for $\mathbf{p}[4]$ to recover $\mathbf{s}[0]$.
- **Burst Erasure Channel**: Finally consider the case when the channel introduces a burst of length $B = 3$. In particular suppose that $\mathbf{x}[0]$, $\mathbf{x}[1]$ and $\mathbf{x}[2]$ are erased. The $(4,2)$ RS code will not be able to recover $\mathbf{s}[0]$ and $\mathbf{s}[1]$, although $\mathbf{s}[2]$ can still be recovered from $\mathbf{p}[4]$. In contrast the $(6,3)$ RS code successfully recovers all the erased source packets with a maximum delay of $T = 5$.

Generally speaking, longer block codes in the streaming setup will correct from longer bursts but at the expense of longer delay. However, the size of each block must be small due to the delay constraints. Such an approach significantly limits the error correction capability. As we will see the use of convolutional codes is more desirable than block codes, as it enables the decoder to recover from shorter bursts with smaller delays while longer bursts can be recovered with longer delays. However, before discussing these, we will briefly discuss Rateless codes.

C. Rateless Codes

Reed-Solomon codes exist over fields of sizes at least as large as the block length. Typical block lengths for RS codes are restricted to $n \leq 255$. Rateless codes (e.g., LT codes [9] and Raptor codes [10]) are a class of binary codes that can support considerably longer block lengths which achieve near optimal error correction and are amenable to extremely efficient decoding algorithms. This makes them a natural choice in non-interactive streaming applications. However, since the focus of this paper is on FEC for interactive applications, rateless codes will not be suitable.

D. Random-Linear Convolutional (RLC) Codes

Together with block codes and rateless codes, convolutional codes [16], [18] form a commonly implemented class of error-correcting codes. Such codes have an inherent sequential encoding structure. At each time instant t, a (n, k, m) convolutional code generates one channel packet $\mathbf{x}[t]$ of size n which is a causal combination of the previous m source packets and the current packet, i.e., $\mathbf{x}[t] = f_t(\mathbf{s}[t-m], \ldots, \mathbf{s}[t-1], \mathbf{s}[t])$. The rate of such a code is given by $R = k/n$ and its redundancy is $100(n-k)/k\%$. The code is said to be systematic if each channel packet $\mathbf{x}[t]$ contains the source packet $\mathbf{s}[t]$, i.e., $\mathbf{x}[t] = (\mathbf{s}[t], \mathbf{p}[t])$ where $\mathbf{p}[t]$ is the size $n-k$ parity-check packet at time t. An important class of convolutional codes are linear, time-invariant, convolutional codes, where the parity-check packets can be expressed as

$$\mathbf{p}[t] = \sum_{i=1}^{m} \mathbf{s}[t-i] \cdot \mathbf{H}_i \tag{4}$$

where m denotes the memory of the code and the matrices $\mathbf{H}_i$ are of dimension $k \times n-k$ for each $i = 1, \ldots m$. We note that the summation in (4) starts at $i = 1$ and not $i = 0$, i.e., $\mathbf{p}[t]$ does not combine $\mathbf{s}[t]$ because the packet erasure channel considered will erase $\mathbf{p}[t]$ whenever $\mathbf{s}[t]$ is erased. Furthermore, when $\mathbf{x}[t]$ is not erased, the systematic code will recover $\mathbf{s}[t]$ directly without the need of $\mathbf{p}[t]$.

If the coefficients in the matrix $\mathbf{H}_i$ are selected at random, then the codes are said to be *random-linear convolutional codes*, see e.g., [19], [20]. Such codes guarantee that, with high probability, each parity-check symbol provides an independent equation involving the source symbols. One can also construct the matrices $\mathbf{H}_i$ in a deterministic fashion to satisfy this property. Such constructions also achieve the largest distance up to the code memory and are referred to as Strongly-MDS codes, see e.g., [21], [22]. For simplicity we will refer to all these constructions as RLC Codes.

Fig. 6 illustrates a $(2, 1, 5)$ RLC code of rate $1/2$. In this special case the parity-check packets are the same size as the source packets. We can express

$$\mathbf{p}[t] = \sum_{i=1}^{5} \alpha_i \cdot \mathbf{s}[t-i], \tag{5}$$

where α_i are scalars instead of matrices in (4). We analyze the performance of these codes for the same set of erasure patterns as in the case of block codes.

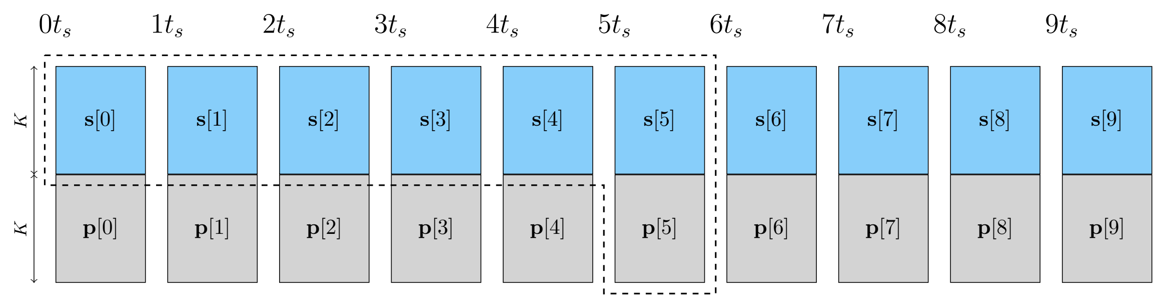

$0t_s$ $1t_s$ $2t_s$ $3t_s$ $4t_s$ $5t_s$ $6t_s$ $7t_s$ $8t_s$ $9t_s$
K
K
$\mathbf{s}[0]$ $\mathbf{s}[1]$ $\mathbf{s}[2]$ $\mathbf{s}[3]$ $\mathbf{s}[4]$ $\mathbf{s}[5]$ $\mathbf{s}[6]$ $\mathbf{s}[7]$ $\mathbf{s}[8]$ $\mathbf{s}[9]$
$\mathbf{p}[0]$ $\mathbf{p}[1]$ $\mathbf{p}[2]$ $\mathbf{p}[3]$ $\mathbf{p}[4]$ $\mathbf{p}[5]$ $\mathbf{p}[6]$ $\mathbf{p}[7]$ $\mathbf{p}[8]$ $\mathbf{p}[9]$

(a) Encoder

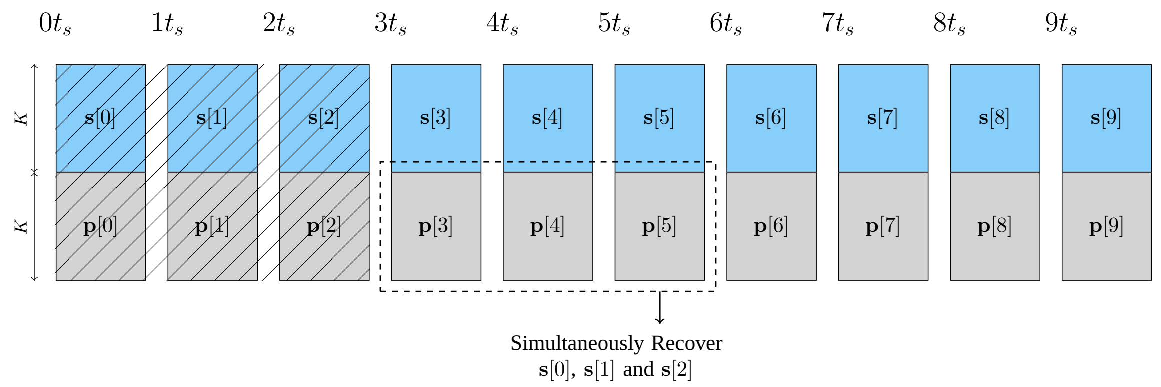

$0t_s$ $1t_s$ $2t_s$ $3t_s$ $4t_s$ $5t_s$ $6t_s$ $7t_s$ $8t_s$ $9t_s$
K
K
$\mathbf{s}[0]$ $\mathbf{s}[1]$ $\mathbf{s}[2]$ $\mathbf{s}[3]$ $\mathbf{s}[4]$ $\mathbf{s}[5]$ $\mathbf{s}[6]$ $\mathbf{s}[7]$ $\mathbf{s}[8]$ $\mathbf{s}[9]$
$\mathbf{p}[0]$ $\mathbf{p}[1]$ $\mathbf{p}[2]$ $\mathbf{p}[3]$ $\mathbf{p}[4]$ $\mathbf{p}[5]$ $\mathbf{p}[6]$ $\mathbf{p}[7]$ $\mathbf{p}[8]$ $\mathbf{p}[9]$
Simultaneously Recover
$\mathbf{s}[0]$, $\mathbf{s}[1]$ and $\mathbf{s}[2]$

(b) Burst of length 3

Fig. 6: $(2,1,5)$ RLC Code

- **Single Isolated Loss**: Consider a channel that introduces a single isolated erasure, i.e., $N = 1$. In particular suppose that $\mathbf{x}[0]$ is lost. It is clear that the erased source packet $\mathbf{s}[0]$ is recovered as soon as the channel packet $\mathbf{x}[1]$ — and in particular, $\mathbf{p}[1]$ — is obtained, i.e., with a delay of $T = 1$ packet. Thus the RLC code achieves a smaller delay than the $(4,2)$ and $(6,3)$ RS codes.
- **Two Isolated Losses**: Next consider the case when the channel introduces up to two isolated losses. It can be verified that the worst case delay occurs when the two losses happen in succession, e.g., if $\mathbf{x}[0]$ and $\mathbf{x}[1]$ are erased. In this case both the source packets $\mathbf{s}[0]$ and $\mathbf{s}[1]$ are recovered when $\mathbf{p}[2]$ and $\mathbf{p}[3]$ are received, i.e., with a delay of $T = 3$. This is the same delay as the shorter $(4,2)$ RS code.
- **Burst Erasure Channel,** $B = 3$: Finally consider the case when the channel introduces a burst of length $B = 3$ and in particular suppose that $\mathbf{x}[0]$, $\mathbf{x}[1]$ and $\mathbf{x}[2]$ are erased. The RLC code will collect the parity-check packets $\mathbf{p}[3], \mathbf{p}[4], \mathbf{p}[5]$ and then recover all the erased source packets — $\mathbf{s}[0], \mathbf{s}[1], \mathbf{s}[2]$ — simultaneously with a delay of $T = 5$. This is illustrated

in Fig. 6b. This is the same delay as the $(6, 3)$ RS code. Furthermore note that since the memory equals $m = 5$, the decoder can also recover a burst of length $B = 4$ with a delay of $T = 7$ and a burst of length $B = 5$ with a delay of $T = 9$. These patterns cannot be corrected by the RS codes discussed previously.

Based on the above discussion, it is clear that convolutional codes exhibit several advantages over block codes. We summarize these below.

- Unlike block codes, convolutional codes do not require the source sequence to be fragmented into blocks over which the parity-checks are generated. Instead they are based on a sliding-window construction (cf. (4)). This approach enables the decoder to opportunistically recover shorter burst lengths more quickly than longer bursts, as we discussed in the above example.
- The memory of the code m is a design parameter. Larger values of m will enable longer burst lengths to be recovered at the same rate. However, longer memory increases complexity and also makes the code vulnerable to certain other types of erasure patterns when partial recovery is the best option. To explain this consider a rate $R = 1/2$ RLC with infinite memory, and one with memory $m = 5$. Suppose the channel introduces a burst of length $B = 20$ in the interval $t \in [i, i+19]$. The infinite-memory code will force the decoder to use the next 20 parity-checks in the interval $[i+20, i+39]$ to recover the erased source sequence. Any additional losses in this period will cause longer delays. The code with memory $m = 5$ will behave very differently. It will skip parity-checks in the interval $[i + 20, i + 24]$, which are the only received parities that depend on the burst interval. Thereafter any parity-checks can be used to recover from any future losses. Thus due to delay constraints the code with memory $m = 5$ is more desirable in the event of such burst losses.

It should be noted that the construction in (4) applies to any arbitrary rate R. There is nothing special about $R = 1/2$, except the simple construction (5). The following result shows the burst and isolated error correction properties of RLC [13] for an arbitrary rate R.

Theorem 1 (Error correction properties of RLC at a given maximum delay)**.** *Consider a (n, k, m) RLC code with rate $R = \frac{k}{n}$ and memory $m \geq T$. Such a code can recover from a burst erasure channel with maximum burst length B, or from an isolated erasure channel with a maximum of*

N erasures, with a maximum delay of T, provided that:

$$B \leq (1-R)(T+1), \tag{6}$$

$$N \leq (1-R)(T+1). \tag{7}$$

Note that RLC codes have the same threshold for burst error and isolated error correction. To explain this, recall that RLC codes perform simultaneous recovery of the source packets in the event of an erasure burst. They treat each parity-check as providing an equation involving the source symbols and recover all the erased symbols simultaneously when sufficiently many parity-checks are received. This is illustrated in Fig. 6b. They are not able to recover earlier source packets whose deadlines happen earlier in an opportunistic fashion. In Sections II-E—II-H we will discuss the class of streaming codes that can achieve such a sequential recovery, and thus provide improved performance over burst erasure channels.

E. Shifted-Repetition Code

A repetition code is a simple construction with rate $R = 1/2$, where each source packet is repeated with a unit delay, i.e., $\mathbf{x}[i] = (\mathbf{s}[i], \mathbf{s}[i-1])$ for all $i \geq 1$. While simple in implementation, such a construction cannot recover from burst losses of length $B \geq 2$. Interestingly a simple variation of this construction achieves optimal recovery over the burst erasure channel. Some generalizations of repetition codes, where low bit rate redundant audio packets are used as parities, are studied in [23].

A shifted-Repetition code is a rate $R = 1/2$ code, where each source packet is repeated once after a delay of T packets, i.e., we can express $\mathbf{x}[i] = (\mathbf{s}[i], \mathbf{s}[i-T])$. Note that in contrast to RLC, the parity-check packets in a shifted-Repetition code do not involve a linear combination of the source packets. We replace (4) with simply $\mathbf{p}[i] = \mathbf{s}[i-5]$. We note the following properties:

- **Single Isolated Loss**: When there is a single isolated loss the corresponding source packet can be recovered with a delay of $T = 5$ packets. For example if $\mathbf{x}[0]$ is lost then the source packet $\mathbf{s}[0]$ is recovered when its repeated copy at time $T = 5$ is received.
- **Two Isolated Losses**: The shifted-Repetition code cannot recover from two or more isolated losses in general. As an example, if the erasures happen at time $t = 0$ and $t = 5$, then the source packet $\mathbf{s}[0]$ cannot be recovered. Thus the delay for this case is ∞.

- **Burst Erasure Channel**: The shifted-Repetition code can correct a burst of length $B = 5$ with a delay of $T = 5$. Suppose that the erasure burst spans the interval $[0, 4]$. Then $\mathbf{s}[0]$ is recovered at time $t = 5$ from $\mathbf{p}[5] = \mathbf{s}[0]$. Likewise each $\mathbf{s}[j]$ for $j = 0, \ldots, 4$ is recovered at time $t = j + 5$ in a sequential manner.

It is clear that a shifted-Repetition code with delay T will recover any burst of length $B \leq T$. This is clearly the maximum burst length that can be recovered by any code. However, the rate of the code is fixed to $R = 1/2$. The family of Maximally Short (MS) codes [24], [25] are a generalization of the shifted-Repetition code that achieve optimal burst correction. For a given rate R and delay T, they achieve $B = \min\left(1, \frac{1-R}{R}\right) T$. We will review a variation of the original construction in Section III. It should be noted that the value of B is larger than that of RLC codes in Theorem 1. Unfortunately like the shifted-Repetition codes, these codes are also sensitive to the isolated erasure channel with $N \geq 2$. We will see that this can lead to a significant degradation over statistical channels such as the Gilbert-Elliott channel. Nevertheless the MS codes constitute an important building block for more robust codes discussed in the sequel.

F. Shifted Random Linear Convolutional Code

Shifted-RLC codes combine ideas of the shifted-Repetition code discussed above with the RLC code in Section II-D. They achieve a longer burst-error correction threshold than RLC codes in Theorem 1, but smaller than the shifted-Repetition codes. However, they can correct from more than one isolated loss unlike the shifted-Repetition codes. As an example consider the rate $1/2$ code: $\mathbf{x}[i] = (\mathbf{s}[i], \mathbf{p}[i])$, where we select

$$\mathbf{p}[i] = \mathbf{s}[i-5] + \mathbf{s}[i-4].$$

This code is similar to the $(n = 2, k = 1, m = 2)$ RLC code in Section II-D, but the parity-check packets are further delayed by $\Delta = 3$ units. We summarize the error correction properties below.

- **Single Isolated Loss**: When there is a single isolated loss the corresponding source packet can be recovered with a delay of $T = 4$ packets. For example if $\mathbf{x}[0]$ is erased, $\mathbf{s}[0]$ is recovered when $\mathbf{p}[4] = \mathbf{s}[0] + \mathbf{s}[-1]$ is available to the decoder.
- **Two Isolated Losses**: This code recovers from any pattern consisting of $N = 2$ erasures within a worst case delay of $T = 5$. The worst case pattern corresponds to $\mathbf{x}[0]$ and $\mathbf{x}[4]$

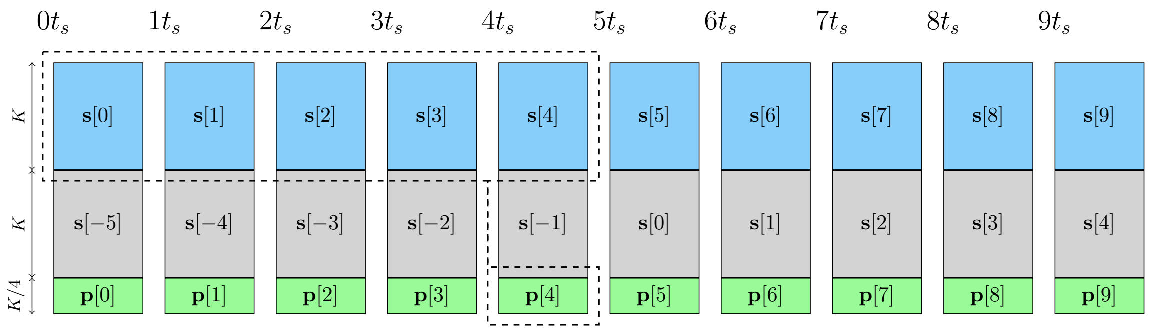

Fig. 7: Rate $4/9$ Concatenated Code

being erased. For this pattern note that the first available parity-check that involves $\mathbf{s}[0]$ is at time $T = 5$. Using $\mathbf{p}[5] = \mathbf{s}[1] + \mathbf{s}[0]$, the source packet $\mathbf{s}[0]$ is recovered at $T = 5$.

- **Burst Erasure Channel**: A burst of length $B \le 4$ packets is recoverable with a delay of $T = 4$. For example, suppose that $\mathbf{x}[0], \ldots, \mathbf{x}[3]$ are erased. Then using $\mathbf{p}[4] = \mathbf{s}[0] + \mathbf{s}[-1]$, and cancelling $\mathbf{s}[-1]$, which is not erased the decoder can recover $\mathbf{s}[0]$. Similarly at time $t = 5$, the decoder can use $\mathbf{p}[5] = \mathbf{s}[0] + \mathbf{s}[1]$ to recover $\mathbf{s}[1]$. Continuing this process, each erased packet is recovered sequentially with delay $T = 4$.

The shifted-RLC code above corrects a maximum burst length of $B = 4$, and up to $N = 2$ isolated losses within a worst case delay of $T = 5$. For the same delay of $T = 5$, the shifted-Repetition code recovers a burst length of $B = 5$, while the RLC code in Theorem 1 can recover from a burst length of $B = 3$, as well as $N = 3$ isolated losses. The main design parameter in the shifted-RLC code is the shift Δ applied to the parity-check packets. Selecting $\Delta = 0$ we recover the original RLC construction and result in the error-correction thresholds stated in Theorem 1. Selecting $\Delta = T$ will result in the same performance as the shifted-Repetition code. By selecting the value of Δ in-between these two extremes we can trade-off the burst-error and isolated-error correction capabilities of the code.

A generalization of the shifted-RLC code above to arbitrary rates is the ERLC [15]. In this construction too, a graceful trade-off between the burst error correction and the isolated error correction capabilities can be obtained through the choice of the shift-parameter Δ. These codes will be reviewed in Section III.

G. Concatenated Codes

An alternative technique for making shifted-Repetition codes resilient to the isolated erasure channel model is to append an extra layer of parity-checks. In Fig. 7, we illustrate an Concatenated code of rate $R = 4/9$ which combines a shifted-Repetition code and a RLC code. The encoding steps are as follows:

- We construct a rate $1/2$ shifted-Repetition code with a delay of $T = 5$. Each source packet $\mathbf{s}[i]$ is repeated with a delay of $T = 5$ as shown.
- We apply a $(n = 5k/4, k, m = 5)$ RLC to the source packet $\mathbf{s}[i]$ to generate parity-check packets of size $k/4$. These parity-check packets are appended to the source packets to generate the channel packet: $\mathbf{x}[i] = (\mathbf{s}[i], \mathbf{s}[i-5], \mathbf{p}[i])$.

The rate of the above construction is $4/9$, which is lower than other codes discussed in this section. The construction of the rate $1/2$ code in this family is a little more complicated. The construction for general rates will be discussed in the subsequent section. Nevertheless this code is effective against burst and isolated erasures as discussed below.

- **Single Isolated Loss**: When there is a single isolated loss the corresponding source packet can be recovered with a delay of $T = 4$ packets. For example if $\mathbf{x}[0]$ is erased, $\mathbf{s}[0]$ is recovered when $\mathbf{p}[1], \ldots \mathbf{p}[4]$ become available using the RLC code. Alternatively, the repetition code can also be used to recover $\mathbf{s}[0]$, albeit with a delay of $T = 5$ packets.
- **Two Isolated Losses**: This code recovers from $N = 2$ isolated erasures within a worst case delay $T = 5$. The worst case pattern corresponds to an erasure at $t = 0$ and an additional erasure in the interval $[1, 4]$. This will force the decoder to use the repetition code to recover $\mathbf{s}[0]$, resulting in a delay of $T = 5$.
- **Burst Erasure Channel**: A burst of length $B \leq 5$ packets is recoverable with a delay of $T = 5$ by simply using the shifted-Repetition constituent code, and ignoring the RLC.

For the burst erasure channels, the Concatenated code above recovers from the same burst lengths as the shifted-repetition code. For the isolated erasure channel, it has the same performance as the shifted-RLC. However, the rate of this code is $R = 4/9$, which is smaller than the other codes that achieve $R = 1/2$. A generalization of this approach to arbitrary rates, known as the MIDAS code, is introduced in [13], [14]. Similarly, this construction is obtained through an extension of MS codes by appending an extra layer of RLC parity-checks as will be explained in Section III.

H. Dual-Delay Codes

Although Shifted-RLC and Concatenated codes in Sections II-F and II-G can recover from both isolated and burst erasures, they incur long delays even in the case of a single erasure. In this section, we discuss another construction that quickly recovers from a single erasure while keeping a good burst correction capabilities. The rate $1/2$ version of such codes is a simple combination of two shifted-Repetition codes with delays of 1 and 5, i.e., the parity-check packet at time i is given by

$$\mathbf{p}[i] = \mathbf{s}[i-1] + \mathbf{s}[i-5].$$

The achievable recovery delays for different erasure patterns are as follows.

- **Single Isolated Loss**: In case of a single erasure, the corresponding packet can be recovered with a delay of $T = 1$ packet. For example if $\mathbf{x}[0]$ is erased, $\mathbf{s}[0]$ is recovered at time 1 since $\mathbf{p}[1] = \mathbf{s}[0] + \mathbf{s}[-4]$.
- **Two Isolated Losses**: This code recovers from $N = 2$ isolated erasures within a worst case delay $T = 5$. The worst case pattern corresponds to two consecutive erasures at time 0 and 1. The decoder has to wait till $\mathbf{p}[5] = \mathbf{s}[4] + \mathbf{s}[0]$ becomes available.
- **Burst Erasure Channel**: A burst of length $B = 4$ packets is recoverable with a delay of $T = 5$. In this case, the parities $\mathbf{p}[5], \ldots, \mathbf{p}[8]$ can be used to recover the erased $\mathbf{s}[0], \ldots, \mathbf{s}[3]$, respectively.

Unlike other constructions, this code is still under investigation and will not be treated further.

I. Numerical Comparisons

Table I summarizes the properties of various error correction codes discussed in the previous section. We set the worst-case delay of each code to be at most $T = 5$ and find the maximum burst length that can be corrected by each. All codes except the Concatenated code have a rate of $R = 1/2$. The rate of the Concatenated code is $R = 4/9$. Note that the shifted-Repetition code achieves the maximum value of $B = 5$, among all codes. However, it cannot recover from the isolated erasure channel with $N \geq 2$. For such a channel, the RLC codes clearly outperform

Error Correction Code	Rate (Redundancy)	Burst $B_{\max}$	Burst T_{worst}	Single Erasure T_{worst}	Two Erasures T_{worst}
$(6,3)$ Reed-Solomon	$1/2$ (100%)	3	5	3	4
RLC Code	$1/2$ (100%)	3	5	1	3
Shifted-Repetition (Maximally Short)	$1/2$ (100%)	5	5	5	∞
Shifted-RLC (Embedded-RLC)	$1/2$ (100%)	4	4	4	5
Concatenated Code (MIDAS)	$4/9$ (125%)	5	5	4	5
Dual-Delay Code	$1/2$ (100%)	4	5	1	5

TABLE I: Summary of error correction codes discussed in Section II. We assume a maximum recovery delay of $T = 5$ for the burst erasure channel and compute the maximum correctable burst length. We also indicate the achievable delays over the isolated erasure channel with $N = 1$ and $N = 2$ erasures. The codes indicated in the parenthesis are generalizations of the codes discussed in this section.

all other codes. However, they can only correct a burst of length $B = 3$. The shifted-RLC code and the Concatenated code achieve $B = 4$, and are also feasible against isolated erasures, albeit with higher delays than RLC codes.

We further compare the performance of these codes at $T = 5$ over Gilbert-Elliott channels and real packet traces in Section V.

J. *Impact on Applications*

As noted before, the maximum allowable one-way latency in interactive applications should not exceed 150 ms. In a VoIP application where each audio packet spans 10 or 20 ms of speech, and assuming $30 - 40$ ms propagation delay for coast-to-coast communication [4], this corresponds to a maximum allowed delay of $T = 5$ to 12 packets. In a typical video application at 2 Mbps, and packet sizes of 1500 Bytes, a delay of $150 - 30 = 120$ ms will be $T \approx 20$ packets [15].

The codes in Table I can be naturally extended to recover from an arbitrary burst length B and delay T. Fig. 8 provides an extension of Fig. 4 to include the robust extensions. The uppermost black line corresponds to RLC while the lowermost red line corresponds to shifted-Repetition (MS) codes as before. Codes such as shifted-RLC (ERLC) and Concatenated Codes (MIDAS) require a slightly larger delay for burst-error correction, but are also robust to isolated losses. We note that the rate is set to be $R = 1/2$ for all codes in Fig. 8. As an example, consider $B = 11$. We observe that the delay achieved by an RLC code equals $T = 21$, while the shifted-Repetition

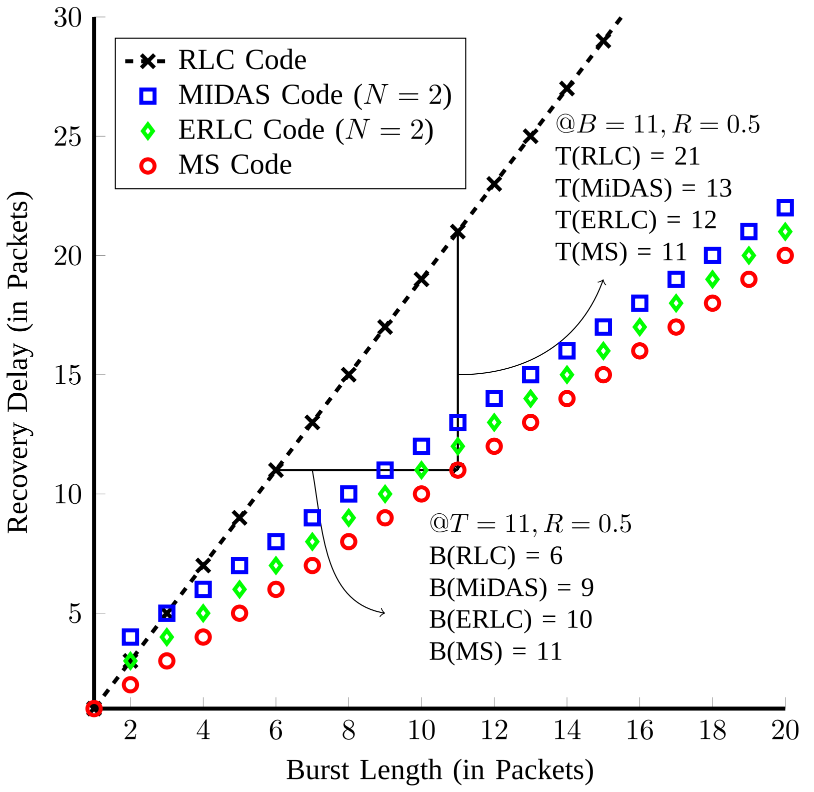

Fig. 8: Achievable recovery delays for different burst lengths using FEC at rate $1/2$. Sequential recovery codes (such as Maximally Short Codes) incur a much lower delay when compared to simultaneous recovery codes (such as Reed-Solomon codes and Random Linear Convolutonal Codes) for a given burst length.

(MS) code achieves $T = 11$. The two robust extensions, which can both correct from $N = 2$ isolated erasures, require only a slightly larger delay. Similarly, if we look at a recovery delay of $T = 11$, we see that the streaming codes — shifted-Repetition (MS), shifted-RLC (ERLC) and Concatenated (MIDAS) codes — can recover from bursts of lengths 11, 10 and 9, respectively compared to a $B = 6$ for the RLC code of the same redundancy.

We conclude by noting that while this section considers very simple channel models throughout the discussion, the insights gleaned from this study are valuable over more realistic channel models. This will be validated in Section V where we show how the streaming codes can outperform conventional codes over Gilbert-Elliott channels as well as real packet traces.

III. General Code Constructions

In this section we extend the streaming code constructions discussed in the previous section to general parameters. We first discuss the Maximally Short Codes in Section III-A. Recall that these codes are a generalization of the shifted-Repetition codes discussed in Section II-E. These codes achieve optimal error correction over the burst erasure channel. However, they cannot recover from even $N = 2$ isolated erasures. We then outline two approaches — the ERLC code and the MIDAS code — that are also robust to isolated losses.

A. Maximally Short (MS) Codes

The MS codes were introduced in [24], [25] and shown to achieve maximum burst correction capability for a given rate and delay. The original constructions of MS codes in [24], [25] were based upon interleaved block codes. A modification was suggested in [13] that did not use the block code construction. Instead, the MS code was constructed using a RLC code and a repetition code as constituent codes. We will follow this approach as it is simpler to describe and generalizes naturally to the robust extensions.

Before explaining the detailed construction, we outline intuition behind the construction of the MS code. The shifted-Repetition code in Section II-E is an *intra-packet code*. It does not combine symbols belonging to different source packets. It sequentially recovers the source packets, but its rate is fixed to $1/2$. The *RLC code* in Section II-D is an *inter-packet code* as it combines symbols across different source packets (4). This construction allows for a flexible rate-delay trade-off but only achieves simultaneous recovery. In the MS code construction we combine the contributions of both the RLC code and the repetition code as illustrated in Fig. 9.

Encoder:

- **Source Splitting:** Split each source packet into two sub-packets $\mathbf{u}[i]$ and $\mathbf{v}[i]$ of sizes K_u and K_v, respectively, where $K_u + K_v = K$, i.e.,

$$\mathbf{s}[i] = (\mathbf{u}[i], \mathbf{v}[i]).$$

- **RLC Code:** Apply a rate $K_v/(K_v + K_u)$ RLC code to the $\mathbf{v}[\cdot]$ stream of sub-packets to generate parity-check packets, $\mathbf{p}_v[\cdot]$ of size K_u.
- **Repetition Code:** Apply a shifted-repetition code to the $\mathbf{u}[\cdot]$ sub-packets.
- **Parity Combination:** Combine the $\mathbf{p}_v[\cdot]$ parity-check packets with the repeated $\mathbf{u}[\cdot]$ sub-packets after shifting the latter by T time slots to generate the overall parity-check packets,

$$\mathbf{p}[i] = \mathbf{p}_v[i] + \mathbf{u}[i - T].$$

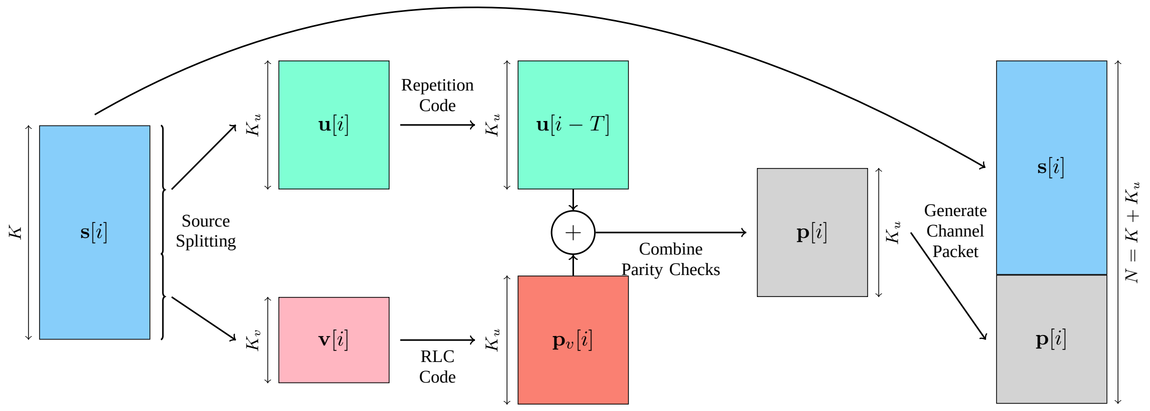

Fig. 9: A block diagram illustrating the encoding steps of a MS code. The source packet is first split into two sub-packets and a different code is applied to each sub-packet. The resulting parity-checks are then combined to form the overall parity-check packet. Finally, the parity-check packet is appended to the source packet to generate the channel packet.

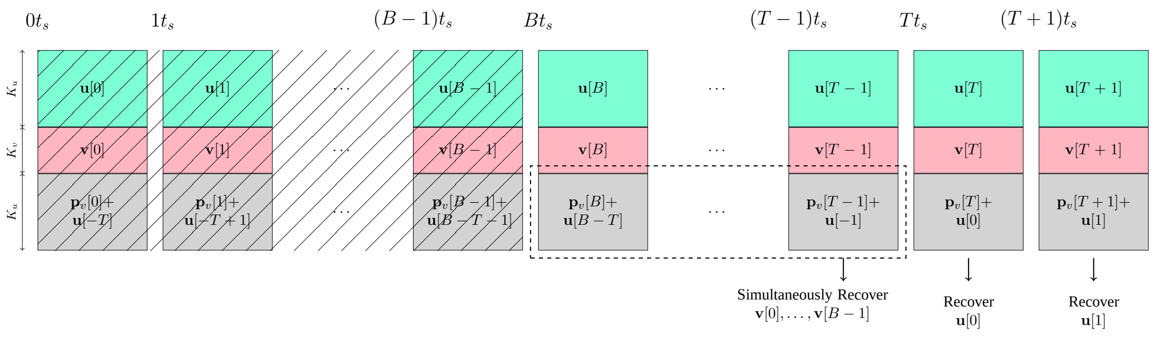

Fig. 10: An illustration of the decoding steps in a MS code. Each column denotes a channel packet transmitted at the time index shown above it.

- **Channel Packet:** Generate the channel packets by appending the overall parity-checks to the source packets, i.e.,

$$\mathbf{x}[i] = (\mathbf{s}[i], \mathbf{p}[i])$$

  is the packet transmitted at time i and is of size $N = K + K_u$.

Rate Analysis: In the above construction we may select any value of K_u and K_v such that their ratio is $K_u/K_v = B/(T-B)$. The overall rate is given by $R = \frac{K_u+K_v}{2K_u+K_v} = \frac{T}{T+B}$. We next explain how the code can recover from a burst of length B with a delay of T.

Decoder: Consider a channel that introduces an erasure burst of length B in the interval $[0, B-1]$ as shown in Fig. 10. The decoder proceeds in two steps.

- **Step I:** (Simultaneous Recovery) The decoder subtracts the unerased $\mathbf{u}[B-T],\dots,\mathbf{u}[-1]$ sub-packets from the corresponding parities, $\mathbf{p}[B],\dots,\mathbf{p}[T-1]$ to recover the parity-check packets, $\mathbf{p}_v[B],\dots,\mathbf{p}_v[T-1]$. These $T-B$ parities, each consisting of K_u symbols, suffice to recover the B erased $\mathbf{v}[\cdot]$ symbols since $B\cdot K_v = (T-B)\cdot K_u$ holds.
- **Step II:** (Sequential Recovery) Upon recovering $\mathbf{v}[0],\dots,\mathbf{v}[B-1]$ at time $T-1$, the decoder can compute $\mathbf{p}_v[T]$, subtract it from $\mathbf{p}[T]=\mathbf{p}_v[T]+\mathbf{u}[0]$ and in turn recover $\mathbf{u}[0]$ at time T. Similarly, the decoder can use $\mathbf{p}[T+1],\dots,\mathbf{p}[T+B-1]$ to sequentially recover $\mathbf{u}[1],\dots,\mathbf{u}[B-1]$ with a delay of T packets.

Hence, $\mathbf{s}[i]=(\mathbf{u}[i],\mathbf{v}[i])$ for $i\in\{0,\dots,B-1\}$ are recovered at time $i+T$.

We summarize the error correction property of the MS code below [24], [25] .

Theorem 2 (Error correction properties of MS codes at a given maximum delay)**.** *Given a rate R and delay T, the MS code can recover from a burst erasure channel of maximum length B or an isolated erasure channel with N erasures provided that:*

$$B \le \min\left(1, \frac{1-R}{R}\right) T \tag{8}$$

$$N \le 1 \tag{9}$$

Furthermore the upper bound on B in (8) *is the maximum value that can be attained by any code of rate R and delay T.*

B. Robust Extensions of MS Codes

As shown in Fig. 10, the MS Code splits the source packet into two groups, i.e., $\mathbf{s}[i]=(\mathbf{u}[i],\mathbf{v}[i])$. It applies a shifted-Repetition code to $\mathbf{u}[i]$ and a RLC code to $\mathbf{v}[i]$ to generate the parity-check packet $\mathbf{p}_v[i]+\mathbf{u}[i-T]$. The main weakness of this construction is the shifted-Repetition code applied to the $\mathbf{u}[\cdot]$ packets. When there are two isolated losses, at time $t=0$ and $t=T$, the MS code fails to recover the sub-packet $\mathbf{u}[0]$. We discuss two ways in which these codes can be made robust to correct from isolated losses.

1) Maximum Distance and Span (MIDAS) Codes : The main idea in the MIDAS construction is to apply an additional RLC code of rate $\frac{K_u}{K_u+K_r}$ to the $\mathbf{u}[i]$ sub-packets. This generates a new-set of parity-check packets $\mathbf{p}_u[i]$ consisting of K_r symbols. These are then appended to the MS code. Thus the transmitted channel packet is of the form $\mathbf{x}[i]=(\mathbf{u}[i],\mathbf{v}[i],\mathbf{u}[i-T]+\mathbf{p}_v[i],\mathbf{p}_u[i])$.

By judiciously selecting K_r one can achieve any $N \leq B$, see [13] . Note that this construction is a generalization of the Concatenated Code discussed in the previous section. The following result from [13] characterizes the performance of these codes.

Theorem 3 (Error correction properties of MIDAS codes at a given maximum delay)**.** *Given a rate R and delay T, there exists a MIDAS code that can recover from a burst erasure channel of maximum length B or an isolated erasure channel with N erasures provided that B and N with $1 \leq N \leq B$, satisfy the following inequality:*

$$\left(\frac{R}{1-R}\right) B + N \leq T. \tag{10}$$

Unlike the case of RLC codes in Theorem 1 where $N = B$ and the case of MS codes in Theorem 2 where $N = 1$, the family of MIDAS codes can achieve any value of $N \in [1, B]$ in Theorem 3. Eq. (10) governs the trade-off between the burst-error and isolated-error correction capabilities of MIDAS codes for a given rate and delay. As the value of N increases the value of B must decrease and vice versa. Finally it is also established [13] that the trade-off in (10) is within one unit of the optimal delay.

2) Embedded-Random Linear Codes: In this approach we replace the repetition code in MS with a RLC code. As with the MS codes, we split the source packet $\mathbf{s}[i] = (\mathbf{u}[i], \mathbf{v}[i])$ of size K_u and K_v symbols respectively. We apply a RLC code to the $\mathbf{v}[i]$ packets as before to generate parity-checks $\mathbf{p}_v[i]$ consisting of K_u symbols. We however substitute the rate-$1/2$ repetition code applied to the $\mathbf{u}[i]$ packets with a rate-$1/2$ RLC code to generate parity-check packets $\mathbf{p}_u[i]$ consisting of K_u symbols. The channel packet transmitted at time i is expressed as $\mathbf{x}[i] = (\mathbf{u}[i], \mathbf{v}[i], \mathbf{p}_v[i] + \mathbf{p}_u[i - \Delta])$, where $\Delta \in [0, T]$ denotes the shift applied the $\mathbf{p}_u[\cdot]$ stream. By judiciously selecting the value of Δ we can trade-off the burst error correction and the isolated error correction capability of this code [15].

Theorem 4 (Error correction properties of ERLC at a given maximum delay)**.** *Consider an ERLC code of rate R, delay T and shift Δ that satisfies $\Delta \geq R(T+1)$. For $R \geq 1/2$, the ERLC code can recover from a burst erasure channel with maximum burst length B, or an isolated erasure* *channel with a maximum of N erasures provided that:*

$$B \leq \frac{1-R}{R}\Delta, \tag{11}$$

$$N \leq \frac{1-R}{R}(T-\Delta)+1. \tag{12}$$

Remark 3. *In the ERLC construction the choice of the shift Δ is a design parameter. By varying the value of Δ, we can attain a trade-off between the burst-error and isolated-error correction capabilities of the code [15].*

From Theorems 4 and 3, at rate $R = 1/2$, ERLC codes achieve larger values of B and N than MIDAS at a given T. ERLC codes are also shown to outperform MIDAS codes on patterns consisting of a burst followed by isolated losses (cf. [14]). We will see that these advantages of the ERLC codes also lead to improved performance in simulations over the statistical channel models. But before presenting the simulation results we provide a survey of the existing literature on Streaming Codes.

IV. Literature Survey

Having discussed some of the basic streaming code constructions in the previous sections, we provide a survey of existing literature in this area. In the broader literature there has been a long-standing interest in packet-level convolutional codes for burst-error correction; see [21], [26]–[30] and the references therein. However, these references do not impose the decoding delay constraint and focus only on error recovery. The streaming setup in Fig. 2 was introduced, to our knowledge, by Martinian and Sundberg [24]. The class of Maximally Short codes (MS) codes for the burst erasure channel that we discussed in Section III-A were also presented in [24]. These were further developed in [20], [25], where explicit code constructions were provided for all feasible burst lengths and decoding delays. The construction in these works were based on a two stage approach. A low delay block code was first constructed and then interleaved to construct a convolutional code. Later, reference [13] provided an alternative approach that did not require the block code construction, but directly constructed the convolutional code using a RLC code and a repetition code as constituent codes. This approach was outlined in Section III-A.

While MS codes achieve the optimal burst erasure correction capability they are sensitive to other loss patterns. In [13]–[15], a sliding window channel model with burst and isolated erasures is introduced and the MIDAS and ERLC codes are introduced these works. A fundamental trade-off between the burst erasure and isolated erasure correction properties of any code is established. This framework is used to establish certain optimality properties of the proposed codes. Our discussion of MIDAS and ERLC codes in Section III-B is based on these references.

Throughout this tutorial paper we restrict our attention to the case when one source packet arrives in each time-slot and one channel packet must be transmitted in each slot. References [13], [31]–[33] consider the case where the source arrival and channel transmission rates are mismatched. In particular, $M > 1$ channel packets must be transmitted by the encoder between two successive source packets. References [13], [31] consider the decoding delay in terms of the source packets and characterize the capacity for the case of burst erasure channels. The associated code constructions are also based on layering scheme like the MS constructions. The optimality of these codes is established for the burst erasure channel model. References [32], [33] study a similar setup when the decoding delay is with respect to channel packets. For the burst erasure model, diagonally interleaved block codes are shown to be optimal when gaps between successive bursts are sufficiently small. For the i.i.d. erasure model a family of time-invariant intra-session codes are proposed with a performance that is close to an upper bound.

References [34], [35] consider a model where the transmitter and receiver are connected through multiple parallel links. Each link is assumed to be a burst erasure channel that introduces a burst of maximum length B. The capacity is characterized in some special cases and joint coding across the sub-channels is required to attain the capacity. Reference [36] considers the setup when the channel between the source and destination is modelled using a linear transfer matrix and is subjected to rank losses. Convolutional coding analogs of rank error correcting codes are proposed that maximize a new distance metric known as the maximum column sum rank. In reference [37], the problem of having multiple erasure bursts within each coding block is studied. It is shown that the recovery delay depends not only on the number of bursts within a coding block, but also on whether the source symbols are encoded causally or non-causally.

In other related works, references [38]–[41] study a multicast extension of [24], [25] involving two users and a common source stream. The stronger receiver's channel introduces shorter bursts and in turn, the decoding delay is required to be smaller. The weaker receiver's channel introduces longer bursts and the decoding delay can be longer. Such codes can also be used in applications where the decoding delay can vary based on channel conditions. The construction of these codes involves embedding the parity-checks of two single-user MS codes in a careful manner to simultaneously satisfy the constraints of both receivers

In the broader literature, unequal error protection for multimedia streaming has been widely studied — see e.g., [42]–[44] and references therein. In [45], the authors proposed a new scheme in streaming models with feedback, which combines the benefits of network coding and ARQ by acknowledging degrees of freedom instead of original packets. In [46]–[48], real-time streaming over blockage channels with delayed feedback is studied. A multi-burst transmission protocol is proposed which achieves a non-trivial trade-off between the delay and throughput within this framework.

V. Simulation Results

In this section, we will study the performance of different FEC codes over Gilbert-Elliott channels as well as real packet traces. In our simulations we fix the rate of the code to be $R = 1/2$. In practice error correction may be invoked only on a subset of packets. For example a large fraction of packets in an audio stream correspond to silence periods. These packets clearly do not need error control. Secondly error control may be only adaptively invoked when the channel conditions require it [11]. Such approaches can substantially reduce the overhead from FEC packets. The maximum recovery delay used in this section is $T = 5$ and $T = 12$ as suggested in Section II-J. Furthermore the packet loss rates we consider are in the interval 10^{-3} to 10^{-6}. The former loss rate will result in a playback disruption every few seconds; the latter loss rate will result into a playback disruption only once every half hour or so.

A. Gilbert-Elliott Channel

A Gilbert-Elliott channel is a two-state Markov model. In the “good state” each channel packet is lost with probability ϵ, whereas in the “bad state” each channel packet is lost with probability 1. We note that the average loss rate of the Gilbert-Elliott channel is given by

$$\Pr(\alpha, \beta, \epsilon) = \frac{\beta}{\beta + \alpha}\epsilon + \frac{\alpha}{\alpha + \beta}, \tag{13}$$

where α and β denote the transition probabilities from the good state to the bad state and vice versa. As long as the channel stays in the bad state the channel behaves as a burst erasure channel.

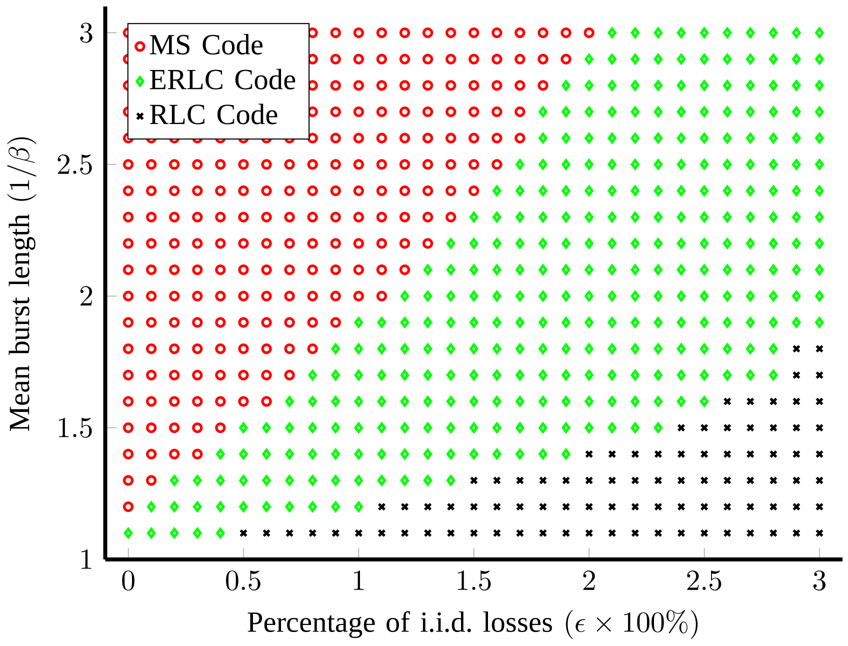

Fig. 11: Numerical comparison over Gilbert-Elliott channel at $\alpha = 5\times10^{-4}$. We vary $\beta \in [1/3, 1)$ to achieve mean burst lengths of $1/\beta$ on the y-axis and $\epsilon \in [0, 3 \times 10^{-2}]$ to achieve i.i.d. loss percentages of 100ϵ % on the x-axis. At each point, we indicate the code that achieves the minimum residual packet loss rate.

The length of each burst is a Geometric random variable of mean $1/\beta$. When the channel is in the good state it behaves as an i.i.d. erasure channel with an erasure probability of ϵ. The gap between two successive bursts is also a geometric random variable with a mean of $1/\alpha$. Finally note that $\epsilon = 0$ results in a Gilbert Channel [49], which results in burst losses only.

In Fig. 11, we fix $\alpha = 5 \times 10^{-4}$ and vary both β and ϵ of the Gilbert-Elliott channel to achieve different mean burst lengths (on the y-axis) and i.i.d. loss rates (on the x-axis). Each point corresponds to a single realization of 10^8 packets. We use rate $R = 1/2$ Shifted-Repetition, Shifted-RLC and RLC codes from Section II-I and set the maximum delay to $T = 5$ packets.

The code with the minimum residual loss rate at a given mean burst length $1/\beta$ and i.i.d. loss percentage 100ϵ is marked in Fig. 11. It turns out that there are three main regions and each code dominates in one. As expected, MS codes outperform other codes when the mean burst lengths are high compared to i.i.d. loss rates between bursts. In the other extreme, RLC codes are the best. Interestingly, ERLC codes which can recover bursts slightly longer than that of RLC codes and more i.i.d. losses compared to MS codes dominate in a region between the two extremes. This shows an application can gainfully switch between the three codes depending on

	Fig. 11		Fig. 12	
α	5×10^{-4}		5×10^{-4}	
β	$[1/3, 1)$		0.4	
ϵ	$[0, 3 \times 10^{-2}]$		$[0, 3 \times 10^{-2}]$	
Channel Length	N/A		5×10^{7}	
Rate R	$1/2$		$1/2$	
Delay T	5		12	
	N	B	N	B
RS	–	–	6	6
RLC	3	3	6	6
MS	1	5	1	12
MIDAS	–	–	2	10
ERLC	2	4	2	11

TABLE II: Channel & Code Parameters used in Simulations. The values of B and N indicate the maximum burst length and the number of isolated losses that can be corrected by each code.

the expected channel characteristics.

Fig. 12 illustrates the results of another experiment over Gilbert-Elliott channels with parameters given in the second column of Table II. We ran simulations over 31 realizations of a Gilbert-Elliott channel each of length 10^8 packets. We set $\alpha = 5 \times 10^{-4}$ and $\beta = 0.4$ in all realizations and vary $\epsilon \in [0, 3] \times 10^{-2}$ across realizations. In Fig. 12, the channel loss rate, $\Pr(\alpha, \beta, \epsilon)$, is plotted on the x-axis, whereas the residual loss probability of different streaming codes is plotted on the y-axis. We assume that the rate of all codes is $R = 1/2$ and the delay is $T = 12$. The achievable values of N and B over the isolated-erasure channel and the burst erasure channels are shown in Table II.

The curves indicated by the black line and marked with '$\times$' correspond to the RLC codes. These codes achieve the largest value of N among all codes in Table II. This explains the relatively constant performance as ϵ is increased. The bottleneck for these codes are long erasure bursts. In particular, note that in Table II these codes achieve a much smaller value of B and hence incur significant packet losses due to long bursts. The curves indicated by light-blue lines and marked with '$+$' correspond to RS block codes. These codes achieve the same value of N and B and hence exhibit a similar pattern to RLC codes. However, as discussed before they are not adaptive and are weaker to non-ideal erasure patterns.

The plots marked with circles, and coloured red, correspond to MS codes. These codes are optimal for the burst erasure channel and achieve the largest value of B among all codes in

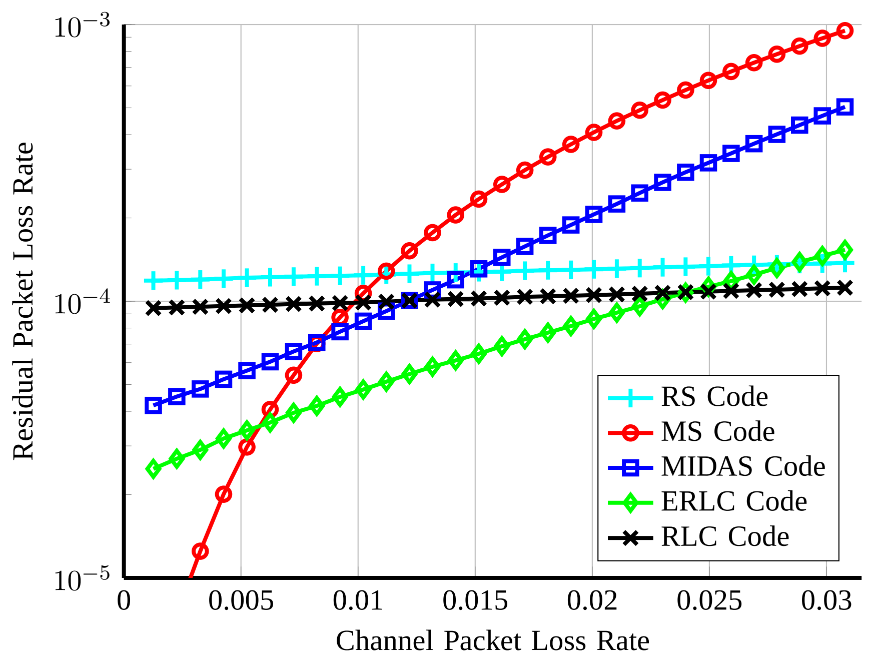

Fig. 12: Simulation over Gilbert-Elliott Channel Model with $(\alpha, \beta, \epsilon) = (5 \times 10^{-4}, 0.4, [0, 0.03])$. The rate for all codes is $R = 1/2$ and the delay is $T = 12$ packets.

Table II. However, they achieve only $N = 1$ and hence the performance is very sensitive to isolated erasures in the good state. In particular, as ϵ increases, the performance deteriorates quickly.

The plots marked with squares, and coloured dark blue/purple, correspond to the MIDAS codes. These codes can balance between the values of B and N and are able to correct both isolated erasures in the good state and longer burst losses in the bad state. MIDAS code combines the advantages of MS and RLC codes.

The plots marked with diamonds and coloured green are the ERLC codes. Similar to MIDAS codes, ERLC codes can balance between the values of B and N. The improvement in loss rate achieved by ERLC codes is due to their capability to partially recover from some non-ideal patterns consisting of burst and isolated erasures in the same decoding window (cf. [14]). Overall, Fig. 12 demonstrates the improvements that different streaming codes can realize over traditional RS and RLC codes.

Fig. 13 studies the effect of increasing delay on different codes. We consider a simulation over the Gilbert-Elliott channel with $\alpha = 5 \times 10^{-4}$, $\beta = 0.4$ and $\epsilon = 4 \times 10^{-3}$. We plot the residual loss-rate of different codes vs. the allowed delay T in the range 5 to 25 packets. At each delay T

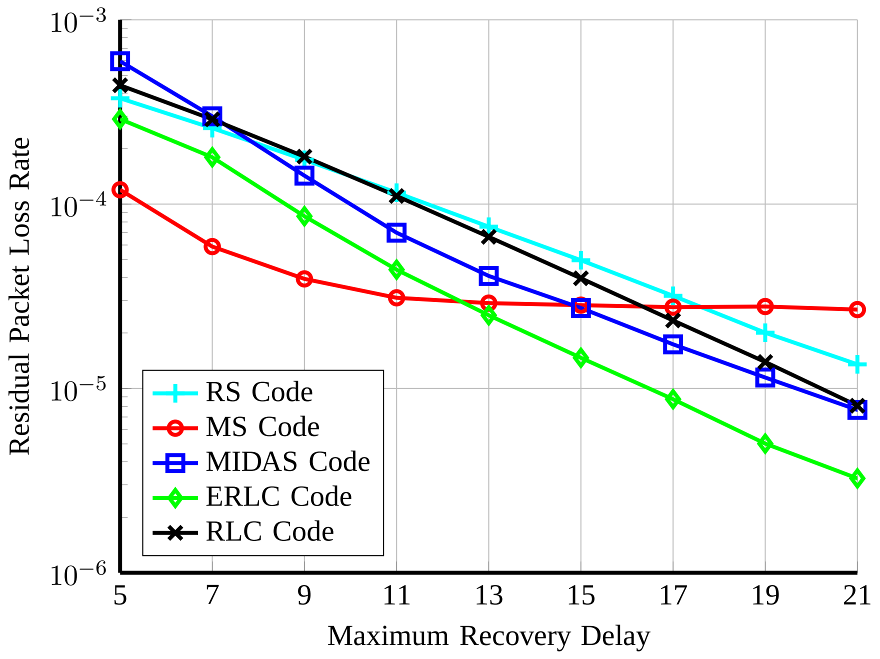

Fig. 13: Simulation Experiments for Gilbert-Elliott Channel Model with $(\alpha, \beta, \epsilon) = (5 \times 10^{-4}, 0.4, 4 \times 10^{-3})$.

and rate $R = 1/2$, RLC and MS codes can achieve only a single pair of (B, N) values, whereas ERLC and MIDAS codes can achieve a set of pairs. The selected pairs – shown in Table III – correspond to the minimum residual loss rate among all pairs. We note that as the allowed delay increases, the isolated erasures and/or burst erasure correction capabilities can be enhanced as shown in Table III. However, only B of the MS code can be increased and not N. Starting at $T = 11$, which corresponds to $B = 11$ for the MS code, its residual loss rate is dominated by the isolated erasure patterns and hence its residual loss rate saturates. On the other hand, as the allowed delay increases, selecting the right values of N and B (cf. Table III) for ERLC and MIDAS codes helps improving their performance over RLC and MS codes which can achieve only a single (B, N) pair for a given T.

B. *Real Packet Traces*

In this section, we validate our results over real packet traces. We simulate the RLC, Shifted-Repetition and Shifted-RLC codes from Sections II-E, II-F and II-D over the dataset in [50]. This dataset consists of over 150 million packets collected over a wireless sensor network while varying multiple parameters, e.g., packet inter-arrival time, payload size, distance between nodes.

Code \ T		5	7	9	11	13	15	17	19	21
RLC Code	B	3	4	5	6	7	8	9	10	11
	N	3	4	5	6	7	8	9	10	11
MS Code	B	5	7	9	11	13	15	17	21	23
	N	1	1	1	1	1	1	1	1	1
MIDAS Code	B	3	5	7	9	11	13	13	14	15
	N	2	2	2	2	2	2	4	5	6
ERLC Code	B	4	6	8	10	12	13	14	14	15
	N	2	2	2	2	2	3	4	6	7

TABLE III: Achievable B and N for different $R = 1/2$ codes, as a function of T, in Fig. 13

We consider packets with inter-arrival time equal to 20 ms since it models most VoIP applications. There are a total of 18.75 million packets with loss rate 8.3%. We use the same codes shown in Fig. 12, whose parameters are indicated in the first column of Table II, and set the delay to $T = 5$ packets or 100 ms. We divide the traces into non-overlapping windows of length 15000 packets each, i.e., 5 minutes of audio. The window length of 15000 packets is chosen to be the approximate coherence time of the channel. Out of the 1250 windows, 133 are loss-free and 139 contain long bursts (> 50 packets). We focus on the remaining 978 windows with moderate mean burst lengths, because we believe the long bursts are due to outages and/or link failures and no FEC can recover from such patterns.

Fig. 14 indicates the code with minimum residual packet loss rate for each of the 978 considered windows. We plot the average non-bursty packet loss rate in each window (sum of isolated losses divided by the length of the window) on the x-axis versus the average burst length in each window (considering any two or more consecutive erasures as a burst) on the y-axis. Interestingly, each of the three simulated codes dominate in a different region.

(a) Windows with short mean burst length (less than 2.5), i.e., close to the x-axis in Fig. 14. In these windows, the isolated losses are the dominant erasure patterns. RLC codes are designed for such channels and achieves the minimum loss rate among all simulated codes.

(b) Windows with small number of isolated packet loss but relatively long mean burst lengths, i.e., top left corner in Fig. 14. Most of the erasures in these windows are due to bursts. Hence the Shifted-Repetition (MS) code, which has the longest burst erasure correction capability $B = 5$, achieves the minimum loss rate in the majority of such windows.

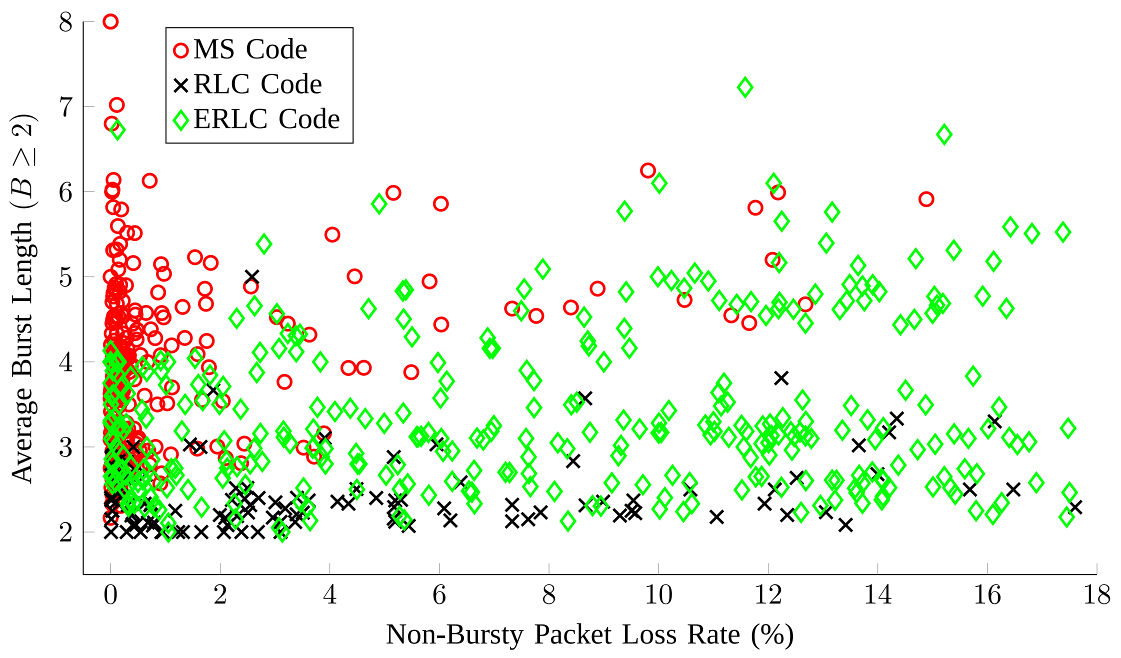

Fig. 14: Simulation results over real packet traces. Each point in the figure corresponds to a window of length 15000 packets with non-bursty packet loss rate on the x-axis and mean burst length on the y-axis. The code that achieves the minimum residual loss rate at each window is indicated with its corresponding mark. These correspond to the first three rows in Table IV.

(c) Windows that introduce relatively balanced mixture of isolated losses as well as long bursts. The Shifted-RLC (ERLC) code, which can recover from a longer burst $B = 4$ compared to that of RLC and more isolated losses $N = 2$ compared to the Shifted-Repetition (MS) code, achieves the minimum loss rate in most of these windows as shown in Fig. 14.

Table IV includes further results of our experiments with these traces. Each row corresponds to a subset of windows where a code of group of codes achieves the minimum residual loss rate. For each subset, we indicate the following:

- Number of windows in the subset;
- The average packet loss rate in these windows;
- The average non-bursty packet loss rate corresponding to isolated losses;
- The average burst length (considering only $B \geq 2$);
- The average of the maximum burst length across windows of the set;
- The average residual loss rates for all three codes, RLC, Shifted-Repetition and Shifted-RLC, in each subset.

The first three rows in Table IV correspond to the points in Fig. 14.

Code with min. PLR	Number of Windows	PLR(%)	Non-Bursty PLR(%)	Mean Burst Length	Maximum Burst Length	Residaul PLR(%)		
						RLC	MS	ERLC
RLC	346	2.43	2.04	2.03	3.14	0.08	0.51	0.10
MS	441	3.72	0.68	3.23	8.15	2.17	1.43	1.71
ERLC	603	5.89	4.49	2.82	5.79	0.91	1.64	0.73
RLC & MS	146	0.09	0.06	1.65	1.82	0.00	0.00	0.00
MS & ERLC	184	0.12	0.05	2.09	2.27	0.02	0.00	0.00
RLC & ERLC	224	0.98	0.88	1.79	2.16	0.02	0.20	0.02
All Codes	142	0.09	0.05	1.62	1.71	0.00	0.00	0.00
Total	978	5.92	3.58	3.10	7.41	1.56	1.79	1.25

TABLE IV: Analysis of the simulations over real packet traces. Each row corresponds to a subset of windows where a code achieves the minimum residual loss rate. The average of the following values across such a subset of windows are also indicated: packet loss rate (PLR), isolated-only packet loss rate, mean burst length, maximum burst length and the residual PLR of each code for such windows.

The values of non-bursty packet loss rate, mean burst length and maximum burst length for different subsets in Table IV confirm the results in Fig. 14. ERLC code achieves the minimum loss rate in more than 60% of the windows considered. It also achieves the minimum average residual loss rate among all 978 windows. However, no single code achieves the best performance for all windows and selecting the right code significantly reduces the residual loss rate in most of the cases. This suggests designing a system that adaptively selects the right code depending on the loss characteristics. According to the considered trace, one can simplify the system by alternating between only two codes. The first is ERLC, which is the best in 603 out of 978 windows $(> 60\%)$. It also achieves a loss rate that is close to that of the best code outside these windows. The second is the MS code, which uniquely achieves the minimum residual loss rate in 253 windows. Most of them lie in the top left corner of Fig. 14 where long bursts are the dominant loss pattern.

Another adaptive approach can use the fact that the ERLC code is a generalization of both MS and RLC codes (cf. Remark 3). Depending on the loss statistics, mean burst length and average loss rate, one can select the right value of the shift Δ for the chosen ERLC code. This includes $\Delta = 0$, $\Delta = 4$ and $\Delta = 5$ which are the RLC, ERLC and MS codes shown in Fig. 14 and Table IV. This will further simplify the system design since a single code will be implemented.

The main conclusion from simulation results over both statistical channels and real packet traces is that no single code achieves the best performance in all cases. However, depending on the loss characteristics, we can estimate which code yields the best performance. Hence, we believe that by tracking the end-to-end delay conditions as well as the loss characteristics during a session, the system can adaptively select the right FEC code and its parameters, e.g., code rate, recovery delay, burst and isolated correction capabilities. Note that the system can in some cases infer the type of bottleneck (e.g., cable modems with drop tail queuing protocol frequently lead to burst losses) which can help make more informed choices about what type of losses to expect in the future and what type of FEC code would be best. Ideally the FEC code and rate would be adapted dynamically throughout a communication session, similar to how the transmitted bit rate is dynamically varied during a session in many video applications today.

VI. Conclusions

Interactive streaming applications require communication systems that achieve low-latency and high reliability in the delivery of source packets. Forward Error Correction codes provide a natural solution to these applications. However, traditional FEC are not designed to satisfy the low-delay and real-time requirements of these applications. As a result many off-the-shelf codes can result in sub-optimal error correction [11].

An exciting opportunity exists to develop new classes of *streaming* codes for interactive streaming application. This tutorial provides a survey of the current state of art constructions of such codes, uses simple illustrative examples to provide insights into these constructions and summarizes the layered design underlying these codes.

We first explain why traditional FEC such as Reed-Solomon Codes, Rateless Codes and Random Linear Convolutional (RLC) Codes are not ideal in streaming applications. These codes do not explicitly consider the different deadlines of different source packets. The resulting code forces the decoder to recover the erased packets simultaneously without taking into account the different decoding deadlines.

We then discuss the class of MS codes that achieve optimal error correction over burst erasure channels by recovering the erased source packets in a sequential fashion. Thus the decoder is capable of recovering older packets with earlier deadlines before the newer packets. These codes correct burst lengths that can be twice as long as traditional codes, or equivalently reduce the recovery delay by up to a factor of two for a given burst length. We then discuss two additional codes — the MIDAS Codes and the ERLC codes — that sacrifice a small amount of burst-error correction capability to achieve significant improvements in robustness over the isolated-erasure channel model. We provide both specific examples and outline general constructions for these codes. We compare their performance over a variety of packet-loss sequences and also demonstrate that they achieve significant gains in simulations over statistical channel models as well as real packet traces.

Many promising future directions are possible. One direction is to design systems that can opportunistically select among different FEC codes depending on the application constraints and the current channel statistics, such as end-to-end delay and loss characteristics. Moreover, designing FEC whose recovery delay adapts to the state of the channel can be beneficial in applications using adaptive play-back techniques. Also, content-aware FEC that adapts to the importance of the source stream can provide improved perceptual quality. Another valuable direction is designing low-delay FEC in case of multiple streams with different delay constraints.

We believe this is a highly promising area for improvement in interactive voice and video communications, augmented and virtual reality applications, and various IoT use cases, and hope that we have conveyed to the reader our excitement about these new opportunities.

References

[1] Cisco White Paper, "Cisco Visual Networking Index: Forecast and Methodology, 2013 - 2018." available online at http://www.cisco.com/, June 2014.

[2] W. Jiang and H. Schulzrinne, "Comparison and optimization of packet loss repair methods on voip perceived quality under bursty loss," in *Proceedings of the 12th international workshop on Network and operating systems support for digital audio and video*, pp. 73–81, ACM, 2002.

[3] Y. J. Liang, J. G. Apostolopoulos, and B. Girod, "Effect of burst losses and correlation between error frames," *IEEE Transactions on Circuits and Systems for Video Technology*, vol. 18, no. 7, 2008.

[4] J. S. Marcus, *Designing wide area networks and internetworks: A practical guide*. Addison-Wesley Professional, 1999.

[5] ITU-T, "G. 114," *One-way transmission time*, vol. 18, 2000.

[6] A. P. Stephens and et al., "IEEE P802.11 wireless LANs: Usage Models, IEEE 802.11-03/802r23," May 2004.

[7] T. Stockhammer and M. Hannuksela, "H.264/AVC video for wireless transmission," *IEEE Wireless Communications*, vol. 12, pp. 6 – 13, aug. 2005.

[8] NSF Workshop on, "Ultra-Low Latency Wireless Networks." available online at http://inlab.lab.asu.edu/nsf/, March 26–27 2015.

[9] M. Luby, "LT codes," in *Proc. Annual IEEE Symposium on Foundations of Computer Science*, 2002.

[10] A. Shokrollahi, "Raptor codes," *IEEE Transactions on Information Theory*, vol. 52, no. 6, pp. 2551–2567, 2006.

[11] T. Huang, P. Huang, K. Chen, and P. Wang, "Could Skype be more satisfying? a QoE-centric study of the FEC mechanism in an internet-scale VoIP system," *IEEE Network*, vol. 24, no. 2, pp. 42–48, 2010.

[12] I. S. Reed and G. Solomon, "Polynomial codes over certain finite fields," *SIAM Journal of Applied Mathematics*, vol. 8, pp. 300 – 304, June 1960.

[13] A. Badr, P. Patil, A. Khisti, W. Tan, and J. Apostolopoulos, "Layered Constructions for Low-Delay Streaming Codes," *IEEE Transactions on Information Theory*, vol. PP, no. 99, pp. 1–1, 2016.

[14] A. Badr, A. Khisti, W. Tan, and J. Apostolopoulos, "Streaming Codes with Partial Recovery over Channels with Burst and Isolated Erasures," *IEEE Journal of Selected Topics in Signal Processing (JSTSP)*, vol. 9, pp. 501–516, April 2015.

[15] A. Badr, A. Khisti, W. Tan, and J. Apostolopoulos, "Streaming Codes for Channels with Burst and Isolated Erasures," 2013.

[16] S. Lin and D. J. Costello, *Error Control Coding: Fundamentals and Applications*. Englewood Cliffs, NJ: Prentice-Hall, 1983.

[17] Z. Li, A. Khisti, and B. Girod, "Forward error protection for low-delay packet video," in *International Packet Video Workshop*, Dec. 2010.

[18] P. Elias, "Coding for noisy channels," *IRE Convention Record*, vol. 4, pp. 37 – 46, Mar. 1955.

[19] G. Joshi, "On playback delay in streaming communication," Master's thesis, Massachusetts Institute of Technology (MIT), 2012.

[20] E. Martinian, *Dynamic Information and Constraints in Source and Channel Coding*. PhD thesis, Massachusetts Institute of Technology (MIT), 2004.

[21] H. Gluesing-Luerssen, J. Rosenthal, and R. Smarandache, "Strongly-MDS Convolutional Codes," *IEEE Transactions on Information Theory*, vol. 52, no. 2, pp. 584–598, 2006.

[22] E. M. Gabidulin, "Convolutional Codes over Large Alphabets," in *Proc. International Workshop on Algebraic Combinatorial and Coding Theory*, (Varna, Bulgaria), pp. 80–84, 1988.

[23] J. C. Bolot, S. Fosse-Parisis, and D. Towsley, "Adaptive FEC-based error control for Internet telephony," vol. 3, pp. 1453–1460 vol.3, Mar 1999.

[24] E. Martinian and C. W. Sundberg, "Burst Erasure Correction Codes with Low Decoding Delay," *IEEE Transactions on Information Theory*, vol. 50, no. 10, pp. 2494–2502, 2004.

[25] E. Martinian and M. Trott, "Delay-optimal burst erasure code construction," in *Proc. International Symposium on Information Theory (ISIT)*, (Nice, France), July 2007.

[26] M. Arai, A. Yamamoto, A. Yamaguchi, S. Fukumoto, and K. Iwasaki, "Analysis of using convolutional codes to recover packet losses over burst erasure channels," in *Dependable Computing, 2001. Proceedings. 2001 Pacific Rim International Symposium on*, pp. 258–265, IEEE, 2001.

[27] H. Deng, M. Kuijper, and J. Evans, "Burst erasure correction capabilities of (n, n-1) convolutional codes," in *Communications, 2009. ICC'09. IEEE International Conference on*, pp. 1–5, IEEE, 2009.

[28] B. M. Kurkoski, P. H. Siegel, and J. K. Wolf, "Analysis of convolutional codes on the erasure channel," in *Information Theory, 2004. ISIT 2004. Proceedings. International Symposium on*, p. 460, IEEE, 2004.

[29] R. Smarandache, H. Gluesing-Luerssen, and J. Rosenthal, "Strongly MDS convolutional codes, a new class

of codes with maximal decoding capability," in *Proc. International Symposium on Information Theory (ISIT)*, pp. 426–, 2002.

[30] V. Tomas, J. Rosenthal, and R. Smarandache, "Decoding of convolutional codes over the erasure channel," *IEEE Transactions on Information Theory*, vol. 58, no. 1, pp. 90–108, 2012.

[31] P. Patil, A. Badr, and A. Khisti, "Delay-optimal streaming codes under source-channel rate mismatch," in *Proc. Asilomar Conference on Signals, Systems & Computers*, 2013.

[32] D. Leong and T. Ho, "Erasure coding for real-time streaming," in *Proc. International Symposium on Information Theory (ISIT)*, 2012.

[33] D. Leong, A. Qureshi, and T. Ho, "On coding for real-time streaming under packet erasures," in *Proc. International Symposium on Information Theory (ISIT)*, 2013.

[34] D. Lui, A. Badr, and A. Khisti, "Streaming codes for a double-link burst erasure channel," in *Proc. Canadian Workshop on Information Theory (CWIT)*, 2011.

[35] D. Lui, "Coding theorems for delay sensitive communication over burst-erasure channels," Master's thesis, University of Toronto, Toronto, ON, Aug. 2011.

[36] R. Mahmood, A. Badr, and A. Khisti, "Convolutional codes with maximum column sum rank for network streaming," in *IEEE International Symposium on Information Theory, ISIT 2015, Hong Kong, China, June 14-19, 2015*, pp. 2271–2275, 2015.

[37] Z. Li, A. Khisti, and B. Girod, "Correcting erasure bursts with minimum decoding delay," in *Proc. Asilomar Conference on Signals, Systems & Computers*, 2011.

[38] A. Khisti and J. Singh, "On multicasting with streaming burst-erasure codes," in *Proc. International Symposium on Information Theory (ISIT)*, 2009.

[39] A. Badr, A. Khisti, and E. Martinian, "Diversity Embedded Streaming erasure Codes (DE-SCo): Constructions and Optimality," *IEEE Journal on Selected Areas in Communications (JSAC)*, vol. 29, pp. 1042–1054, May 2011.

[40] A. Badr, D. Lui, and A. Khisti, "Multicast Streaming Codes (Mu-SCo) for burst erasure channels," in *Proc. Allerton Conference on Communication, Control, and Computing*, 2010.

[41] A. Badr, D. Lui, and A. Khisti, "Streaming codes for multicast over burst erasure channels," *IEEE Transactions on Information Theory*, vol. 61, pp. 4181–4208, Aug 2015.

[42] A. Nafaa, T. Taleb, and L. Murphy, "Forward error correction strategies for media streaming over wireless networks," *Communications Magazine, IEEE*, vol. 46, no. 1, pp. 72–79, 2008.

[43] U. Horn, K. Stuhlmüller, M. Link, and B. Girod, "Robust internet video transmission based on scalable coding and unequal error protection," *Signal Processing: Image Communication*, vol. 15, no. 1, pp. 77–94, 1999.

[44] N. Rahnavard, B. N. Vellambi, and F. Fekri, "Rateless codes with unequal error protection property," *IEEE Transactions on Information Theory*, vol. 53, no. 4, pp. 1521–1532, 2007.

[45] J. K. Sundararajan and D. S. and M. Medard, "ARQ for network coding," in *Proc. International Symposium on Information Theory (ISIT)*, 2008.

[46] H. Yao, Y. Kochman, and G. W. Wornell, "A multi-burst transmission strategy for streaming over blockage channels with long feedback delay," *IEEE Journal on Selected Areas in Communications (JSAC)*, vol. 29, no. 10, pp. 2033–2043, 2011.

[47] Y. K. H. Yao and G. W. Wornell, “On delay in real-time streaming communication systems,” in *Proc. Allerton Conference on Communication, Control, and Computing*, 2010.

[48] G. W. W. H. Yao, Y. Kochman, “Delay-throughput tradeoff for streaming over blockage channels with delayed feedback,” in *Proc. IEEE Military Communications Conference (MILCOM)*, 2010.

[49] E. N. Gilbert, “Capacity of a burst-noise channel,” *Bell Systems Technical Journal*, vol. 39, pp. 1253–1265, Sept. 1960.

[50] S. Fu and Y. Zhang, “CRAWDAD dataset due/packet-delivery (v. 2015-04-01).” Downloaded from http://crawdad.org/due/packet-delivery/20150401/delay, Apr. 2015. traceset: delay.

Ahmed Badr received the B.Sc., M.Sc. and Ph.D. degrees in Electrical & Computer Engineering from Cairo University, Egypt in 2007, Nile University, Egypt in 2009 and University of Toronto, Canada in 2014. From September 2007 to August 2009, he was a Research Assistant in the Wireless Intelligent Networks Center (WINC), Nile University. In September 2009, he was a Research Assistant at the Signals Multimedia and Security Laboratory in University of Toronto. In 2014, he assumed his current position as a Postdoctoral Fellow in University of Toronto. His research interests include information theory, coding theory and real-time communication.

Ashish Khisti received his BASc Degree in EngineeringSciences (Electrical Option) from University of Toronto, and his S.M andPh.D. Degrees in Electrical Engineering from the Massachusetts Instituteof Technology. Between 2009-2015, he was an assistant professor in theElectrical and Computer Engineering department at the University of Toronto.He is presently an associate professor, and holds a Canada Research Chair inthe same department. He is a recipient of an Ontario Early Researcher Award,the Hewlett-Packard Innovation Research Award and the Harold H. Hazenteaching assistant award from MIT. He presently serves as an associate editorfor IEEE TRANSACTIONS ON INFORMATION THEORY and is also a guest editor for the Proceedings of the IEEE (SPECIALISSUE ONSECURE COMMUNICATIONS VIA PHYSICAL-LAYER AND INFORMATION-THEORETIC TECHNIQUES).

Wai-tian Tan received BS from Brown University, MSEE from Stanford University, and PhD from University of California, Berkeley, all in electrical engineering. He was a researcher at Hewlett Packard Laboratories from 2000 to 2013 working on various aspects of multimedia communications and systems. He has been with Cisco Systems since 2013, where he is a principal engineer in the Chief Technology and Architecture Office.

John Apostolopoulos is VP/CTO of the Ciscos Enterprise Segment and leads Ciscos Innovation Labs, covering Internet of Things, wireless, application-aware networking, multimedia networking, indoor-location-based services, and deep learning for visual analytics. Previously, he was Lab Director for the Mobile & Immersive Experience Lab at HP Labs. His work spanned novel mobile devices and sensing, client/cloud multimedia computing, multimedia networking, immersive video conferencing, SDN, and mobile streaming media content delivery networks for all-IP (4G) wireless networks. He was a Consulting Associate Professor at Stanford (2000-09), and frequently lectures at MIT. He received his B.S., M.S., and Ph.D. from MIT.